

GRID DIAGRAMS AND MANOLESCU'S UNORIENTED SKEIN EXACT TRIANGLE FOR KNOT FLOER HOMOLOGY

C.-M. MIKE WONG

ABSTRACT. We re-derive Manolescu's unoriented skein exact triangle for knot Floer homology over \mathbb{F}_2 combinatorially using grid diagrams, and extend it to the case with \mathbb{Z} coefficients by sign refinements. Iteration of the triangle gives a cube of resolutions that converges to the knot Floer homology of an oriented link. Finally, we re-establish the homological σ -thinness of quasi-alternating links.

1. INTRODUCTION

Heegaard Floer homology is first introduced in [OS04b] as an invariant for 3-manifolds, defined using holomorphic disks and Heegaard diagrams. It is extended in [OS04a, Ras03] to give an invariant, *knot Floer homology*, for null-homologous knots in a closed, oriented 3-manifold, which is further generalised in [OS08] to the case of oriented links. Knot Floer homology comes in several flavors; its most usual form, $\widehat{\mathrm{HFK}}(L)$ for an oriented link L , is a bigraded module over $\mathbb{F}_2 = \mathbb{Z}/2\mathbb{Z}$ or \mathbb{Z} , whose Euler characteristic is the Alexander polynomial. For the purposes of this paper, we shall only consider links in S^3 .

In [MOS09, MOST07], a combinatorial description of knot Floer homology over \mathbb{F}_2 is given using *grid diagrams*, which are certain multi-pointed Heegaard diagrams on the torus. In this approach, one can associate a chain complex $C(G)$ to a grid diagram G , and calculate its homology $\widehat{\mathrm{HK}}(G)$. Sign refinements for the boundary map ∂ are also given in [MOST07] in a well-defined manner, allowing the chain complex to be defined over \mathbb{Z} . If G is a grid diagram for a link L of ℓ components, with *grid number* n , then

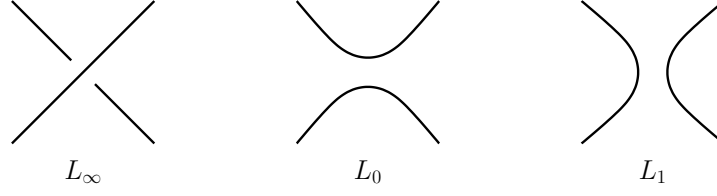
$$\widehat{\mathrm{HK}}(G) \cong \widehat{\mathrm{HFG}}(L) \otimes V^{n-\ell},$$

where V is a free module of rank 2 over the base ring $R = \mathbb{F}_2$ or \mathbb{Z} , and $\widehat{\mathrm{HFG}}(L)$ is a link invariant, called the *combinatorial knot Floer homology* or the *grid homology* of L . Over \mathbb{F}_2 , $\widehat{\mathrm{HFG}}(L)$ is isomorphic to $\widehat{\mathrm{HFK}}(L)$; over \mathbb{Z} , it has been shown in [Sar11] that $\widehat{\mathrm{HFG}}(L)$ is isomorphic to $\widehat{\mathrm{HFK}}(L, \mathfrak{o})$ for some orientation system \mathfrak{o} .

Ozsváth and Szabó observe in [OS05] that, like Khovanov homology $\widehat{\mathrm{Kh}}(L)$ [Kho00, Kho02, BN02], Heegaard Floer homology of the branched double cover $\widehat{\mathrm{HF}}(-\Sigma(L))$ satisfies an unoriented skein exact triangle. Manolescu then shows in [Man07] that over \mathbb{F}_2 , the knot Floer homology also satisfies an unoriented skein exact triangle. More precisely, let L_∞ be a link in S^3 . Given a planar diagram of L_∞ , let L_0 and L_1 be the two resolutions of L_∞ at a crossing in that diagram, as

2010 *Mathematics Subject Classification.* 57R58 (Primary); 57M25, 57M27 (Secondary).

The author was partially supported by the Princeton University Mathematics Department.

FIGURE 1.1. L_∞, L_0 and L_1 near a point.

in Figure 1.1. Denote by $\ell_\infty, \ell_0, \ell_1$ the number of components of the links L_∞, L_0 , and L_1 , respectively, and set $m = \max\{\ell_\infty, \ell_0, \ell_1\}$.

Theorem 1.1 (Manolescu). *Let the base ring be \mathbb{F}_2 . There exists an exact triangle*

$$\cdots \rightarrow \widehat{\text{HFK}}(L_\infty) \otimes V^{m-\ell_\infty} \rightarrow \widehat{\text{HFK}}(L_0) \otimes V^{m-\ell_0} \rightarrow \widehat{\text{HFK}}(L_1) \otimes V^{m-\ell_1} \rightarrow \cdots,$$

where V is a 2-dimensional vector space over \mathbb{F}_2 .

Remark. The arrows in the exact triangle point in the reverse direction from those in [Man07]; this is caused by a difference in the orientation convention. We follow the convention in [OS04a] and [MOS09, MOST07], where the Heegaard surface is the oriented boundary of the handlebody in which the α curves bound discs.

Manolescu remarks that the exact triangle above is different from that of $\widetilde{\text{Kh}}(L)$ and $\widehat{\text{HF}}(-\Sigma(L))$ in that it does not even respect the homological grading modulo 2, and that it is unclear whether an analogous triangle holds for other versions of knot Floer homology. He also uses the exact triangle to show that $\text{rk}_{\mathbb{F}_2} \widehat{\text{HFK}}(L) = 2^{\ell-1} \det(L)$ for quasi-alternating links, which explains the fact that $\widetilde{\text{Kh}}$ and $\widehat{\text{HFK}}$ have equal ranks for many classes of knots.

The goal of the present paper is to re-prove Manolescu's theorem in elementary terms using grid diagrams, without appealing to the topological theory. The advantages of this approach are three-fold.

First, Manolescu's skein exact triangle is proven in [Man07] to exist over \mathbb{F}_2 . By assigning signs to the maps between chain complexes, we can obtain an analogous exact triangle in combinatorial knot Floer homology with \mathbb{Z} coefficients, which has not been known to exist before. In other words, we obtain the following statement.

Theorem 1.2. *Let the base ring be $R = \mathbb{F}_2$ or \mathbb{Z} . There exists an exact triangle*

$$\cdots \rightarrow \widehat{\text{HFG}}(L_\infty) \otimes V^{m-\ell_\infty} \rightarrow \widehat{\text{HFG}}(L_0) \otimes V^{m-\ell_0} \rightarrow \widehat{\text{HFG}}(L_1) \otimes V^{m-\ell_1} \rightarrow \cdots,$$

where V is a free module of rank 2 over R .

Second, the exact triangle is iterated by Baldwin and Levine in [BL12] to obtain a cube of resolutions; when using twisted coefficients, this gives a combinatorial description of knot Floer homology, distinct from that provided by grid diagrams. In the present context, knowing explicitly the maps between the chain complexes associated to the grid diagrams, we can likewise iterate the exact triangle to get a cube of resolutions complex $\text{CR}(G)$, with untwisted coefficients. The higher terms in the resulting spectral sequence are combinatorially computable. Once again, such a spectral sequence over \mathbb{Z} has not been known to exist.

Corollary 1.3. *Let the base ring be $R = \mathbb{F}_2$ or \mathbb{Z} . The cube of resolutions $\text{CR}(G)$ gives rise to a spectral sequence that converges to $\widehat{\text{HFG}}(L) \otimes V^{m-\ell}$.*

The technique of spectral sequences is first used by Ozsváth and Szabó in [OS05], where a spectral sequence from $\widetilde{\text{Kh}}(L)$ to $\widehat{\text{HF}}(\Sigma(L))$ is shown to exist. Recently, Lipshitz, Ozsváth and Thurston have found a way in [LOT] to compute the higher terms in this spectral sequence using bordered Floer homology. Inspired by this work, Baldwin has found another method in [Bal11] of computing these higher terms.

Third, in [MO08], Manolescu and Ozsváth apply the skein exact triangle to *quasi-alternating links*, to show that such links are *Floer homologically σ -thin* over \mathbb{F}_2 . The same can be done in the combinatorial picture; doing so, we prove a generalisation to \mathbb{Z} .

Corollary 1.4. *Let \mathbb{Z} be the base ring. Quasi-alternating links are Floer homologically σ -thin.*

This paper is organised as follows. We review the definition of knot Floer homology in terms of grid diagrams in Section 2, and re-prove the skein exact triangle in Section 3. In these two sections, we will work only over \mathbb{F}_2 . Sign-refinements are then given in Section 4 to establish the analogous result over \mathbb{Z} . Next, we discuss how the exact triangle can be iterated to obtain a cube of resolutions in Section 5. Finally, we establish the homological σ -thinness of quasi-alternating links in Section 6.

Acknowledgements. The author is extremely grateful to John Baldwin for his suggestion of the topic of the paper, and is greatly indebted to John for many essential ideas in the text. The author would also like to thank John Baldwin and Peter Ozsváth for their continuous encouragements and careful guidance throughout the entire research process. Without either of them, this paper would never have been possible. Lastly, the author wishes to thank Ciprian Manolescu for a helpful conversation.

2. GRID DIAGRAMS

We review the combinatorial description of knot Floer homology in terms of grid diagrams. In this and the next section, we will work only over $\mathbb{F}_2 = \mathbb{Z}/2\mathbb{Z}$.

A *planar grid diagram* \tilde{G} with *grid number* n is a square grid in \mathbb{R}^2 with $n \times n$ cells, together with a collection of O 's and X 's, such that

- Each row contains exactly one O and exactly one X ;
- Each column contains exactly one O and exactly one X ; and
- Each cell is either empty, contains one O , or contains one X .

Given a planar grid diagram \tilde{G} , we can place it in a standard position on \mathbb{R}^2 as follows: We place the bottom left corner at the origin, and require that each cell be a square of edge length one. We can then construct an oriented, planar link projection by drawing horizontal segments from the O 's to the X 's in each row, and vertical segments from the X 's to the O 's in each column. At every intersection point, we let the horizontal segment be the underpass and the vertical one the overpass. This gives a planar projection of an oriented link L onto \mathbb{R}^2 ; we say that \tilde{G} is a *planar grid presentation* of L .

We transfer our grid diagram to the torus \mathbb{T} , by gluing the topmost segment to the bottommost one, and gluing the leftmost segment to the rightmost one. Then the horizontal and vertical arcs become horizontal and vertical circles. The torus

inherits its orientation from the plane. The resulting diagram G is a *toroidal grid diagram*, or simply a *grid diagram*. G is then a *grid presentation* of L ; we also say that G is a grid diagram for L .

Given a toroidal grid diagram G , we associate to it a chain complex $(C(G), \partial)$ as follows. The set of generators of $C(G)$, denoted $\mathbf{S}(G)$, consists of one-to-one correspondences between the horizontal and vertical circles. Equivalently, we can regard the generators as n -tuples of intersection points between the horizontal and vertical circles, such that no intersection point appears on more than one horizontal or vertical circle.

We now define the differential map $\partial: C(G) \rightarrow C(G)$. Given $\mathbf{x}, \mathbf{y} \in \mathbf{S}(G)$, let $\text{Rect}(\mathbf{x}, \mathbf{y})$ denote the space of embedded rectangles with the following properties. First of all, $\text{Rect}(\mathbf{x}, \mathbf{y})$ is empty unless \mathbf{x}, \mathbf{y} coincide at exactly $n - 2$ points. An element r of $\text{Rect}(\mathbf{x}, \mathbf{y})$ is an embedded disk in \mathbb{T} , whose boundary consists of four arcs, each contained in horizontal or vertical circles; under the orientation induced on the boundary of r , the horizontal arcs are oriented from a point in \mathbf{x} to a point in \mathbf{y} . The space of empty rectangles $r \in \text{Rect}(\mathbf{x}, \mathbf{y})$ with $\mathbf{x} \cap \text{Int}(r) = \emptyset$ is denoted $\text{Rect}^\circ(\mathbf{x}, \mathbf{y})$.

More generally, a *path* from \mathbf{x} to \mathbf{y} is a 1-cycle γ on \mathbb{T} such that the boundary of the intersection of γ with U_α is $\mathbf{y} - \mathbf{x}$, and a *domain* p from \mathbf{x} to \mathbf{y} is a two-chain in \mathbb{T} whose boundary ∂p is a path from \mathbf{x} to \mathbf{y} ; the set of domains from \mathbf{x} to \mathbf{y} is denoted $\pi(\mathbf{x}, \mathbf{y})$.

Given $\mathbf{x} \in \mathbf{S}(G)$, we define

$$\partial(\mathbf{x}) = \sum_{\mathbf{y} \in \mathbf{S}(G)} \sum_{r \in \text{Rect}^\circ(\mathbf{x}, \mathbf{y})} \left\{ \begin{array}{ll} 1 & \text{if } \text{Int}(r) \text{ contains no } O\text{'s or } X\text{'s} \\ 0 & \text{otherwise} \end{array} \right\} \cdot \mathbf{y} \in C(G).$$

It is not too difficult to see that indeed $\partial \circ \partial = 0$, and so ∂ is a differential: We have

$$\partial \circ \partial(\mathbf{x}) = \sum_{\mathbf{y} \in \mathbf{S}(G)} \sum_{p \in \pi(\mathbf{x}, \mathbf{z})} N(p) \cdot \mathbf{z},$$

where $N(p)$ is the number of ways of decomposing p as a composite of two empty rectangles $p = r_1 * r_2$, where $r_1 \in \text{Rect}^\circ(\mathbf{x}, \mathbf{y})$ and $r_2 \in \text{Rect}^\circ(\mathbf{y}, \mathbf{z})$. Let $p = r_1 * r_2$; then r_1 and r_2 either are disjoint, have overlapping interiors, or share a corner. If r_1 and r_2 are disjoint or have overlapping interiors, then $p = r_2 * r_1$; if they share a corner, then there exists a unique alternate decomposition of $p = r'_1 * r'_2$. In any case, we obtain that $N(p) = 0$ for all $p \in \pi(\mathbf{x}, \mathbf{z})$.

Moreover, to the complex $C(G)$ we can associate a *Maslov grading* and an *Alexander grading*, determined by the functions $M: \mathbf{S} \rightarrow \mathbb{Z}$ and $S: \mathbf{S} \rightarrow \frac{1}{2}\mathbb{Z}$. For reasons we will see in the next section, we will in general not be concerned with these gradings, unless otherwise specified. We postpone their definitions to Section 6. It can be checked, however, that the differential ∂ decreases the Maslov grading by 1 and preserves the Alexander filtration.

We can now take the homology of the chain complex $(C(G), \partial)$, and define

$$\widehat{\text{HK}}(G) = H_*(C(G), \partial).$$

It is shown in [MOS09, MOST07] that, if G is a grid diagram with grid number n for the oriented link L with ℓ components, then

$$\widehat{\text{HK}}(G) \cong \widehat{\text{HK}}(G) \otimes V^{n-\ell},$$

where V is a 2-dimensional vector space over \mathbb{F}_2 , spanned by one generator in (Maslov and Alexander) bigrading $(-1, -1)$ and another in bigrading $(0, 0)$, and $\widehat{\text{HK}}(G)$ is a vector space with

$$\widehat{\text{HK}}(G) \cong \widehat{\text{HFK}}(L).$$

If G is a grid diagram for an oriented link L , then $\widehat{\text{HK}}(G)$ is a link invariant and can also be denoted by $\widehat{\text{HFG}}(L)$, often referred to as the *combinatorial knot Floer homology*, or *grid homology*. $\widehat{\text{HK}}(G)$ can also be denoted by $\widehat{\text{HFG}}(L, n)$.

We end this section with a remark. While the proof that ∂ is a differential is completely elementary, its method is very useful to what we shall prove in this paper. In general, in order to prove that a map defined by counting certain domains is a chain map, or to prove that it is a chain homotopy, we juxtapose two domains and enumerate all possible outcomes.

3. MANOLESCU'S UNORIENTED SKEIN EXACT TRIANGLE

We now reproduce Manolescu's result in purely combinatorial terms.

Before we start our main discussion, we make a change in our notation. In the original description developed in [MOS09, MOST07], the O 's and X 's are used to determine the Alexander and Maslov gradings of the generators. However, given a link L_∞ in S^3 and its two resolutions L_0, L_1 at a crossing, we observe that L_∞, L_0, L_1 do not share a compatible orientation. Since we shall soon combine all three grid diagrams into one, we must forget the orientations of the links; this implies that we must also forget the distinctions between the O 's and X 's, and ignore the gradings. Notice that using only one type of markers will not change the definition of $\widehat{\text{HFG}}(L, n)$, since without the gradings, the definition of the chain complex $C(G)$ associated to a grid diagram G is symmetric in the O 's and the X 's. Therefore, we shall henceforth replace all O 's with X 's.

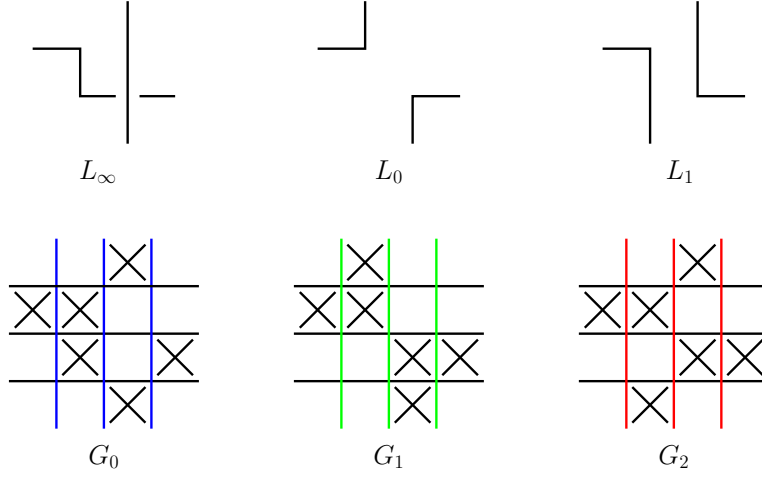
With this new notation, the first two conditions for a grid diagram become the condition that there are exactly two X 's on each row and each column. We denote by \mathbb{X} the set of X 's on a grid diagram. The differential is then given by

$$\partial(\mathbf{x}) = \sum_{\mathbf{y} \in \mathbf{S}(G)} \sum_{\substack{r \in \text{Rect}^o(\mathbf{x}, \mathbf{y}) \\ \text{Int}(r) \cap \mathbb{X} = \emptyset}} \mathbf{y} \in C(G).$$

To begin, we position L_∞, L_0, L_1 as in Figure 3.1, and make sure that their respective grid diagrams G_0, G_1, G_2 are identical except near the crossing, as indicated in the same figure. Next, we let $C_k = C(G_k)$ be the chain complex associated with G_k , for each $k \in \mathbb{Z}/3\mathbb{Z}$.

We remark here that the leftmost and rightmost columns in the diagrams in Figure 3.1 are unnecessary for the rest of our discussion in this and the next section. We leave them in the diagrams in anticipation for an argument in the iteration of the exact triangle in Section 5.

Instead of drawing three different diagrams, we can draw G_0, G_1, G_2 all on the same diagram, as in Figure 3.2. We label by β_k the vertical circle corresponding to G_k , for each $k \in \mathbb{Z}/3\mathbb{Z}$, as indicated. These three vertical circles, together with all the other vertical circles, divide \mathbb{T} into a number of components; we let b be the unique component that is an annulus not containing any X in its interior. Also, exactly three of these components are embedded triangles not containing any X in

FIGURE 3.1. Grid diagrams for L_∞, L_0 and L_1 near a point.

their interior; we let t_k be the triangle whose β_k arc is disjoint from the boundary of b . Finally, β_k and β_{k+1} intersect at exactly two points; we denote by u_k the intersection point that lies on the boundary of b , and by v_k the other intersection point. Then $u_k = b \cap t_{k+2}$ and $v_k = t_k \cap t_{k+1}$.

In this setting and over \mathbb{F}_2 , Theorem 1.2 follows from our main proposition:

Proposition 3.1. *Let the base ring be \mathbb{F}_2 . There exists an exact triangle*

$$\cdots \rightarrow \widetilde{\mathrm{HK}}(G_0) \rightarrow \widetilde{\mathrm{HK}}(G_1) \rightarrow \widetilde{\mathrm{HK}}(G_2) \rightarrow \cdots$$

We make use of the following lemma from homological algebra [OS05], used also in [Man07]:

Lemma 3.2. *Let $\{(C_k, \partial_k)\}_{k \in \mathbb{Z}/3\mathbb{Z}}$ be a collection of chain complexes over \mathbb{F}_2 , and let $\{f_k: C_k \rightarrow C_{k+1}\}_{k \in \mathbb{Z}/3\mathbb{Z}}$ be a collection of chain maps such that the following conditions are satisfied for each k :*

- (1) *The composite $f_{k+1} \circ f_k: C_k \rightarrow C_{k+2}$ is chain-homotopic to zero, by a chain homotopy $\varphi_k: C_k \rightarrow C_{k+2}$:*

$$f_{k+1} \circ f_k + \partial_{k+2} \circ \varphi_k + \varphi_k \circ \partial_k = 0;$$

- (2) *The map $\varphi_{k+1} \circ f_k + f_{k+2} \circ \varphi_k: C_k \rightarrow C_k$ is a quasi-isomorphism. (In particular, if there exists a chain homotopy $\psi_k: C_k \rightarrow C_k$ such that*

$$\varphi_{k+1} \circ f_k + f_{k+2} \circ \varphi_k + \partial_k \circ \psi_k + \psi_k \circ \partial_k = \mathrm{Id},$$

then this condition is satisfied.)

Then the sequence

$$\cdots \rightarrow H_*(C_k) \xrightarrow{(f_k)_*} H_*(C_{k+1}) \xrightarrow{(f_{k+1})_*} H_*(C_{k+2}) \rightarrow \cdots$$

is exact.

We now define the chain maps $f_k: C_k \rightarrow C_{k+1}$ by counting pentagons and triangles.

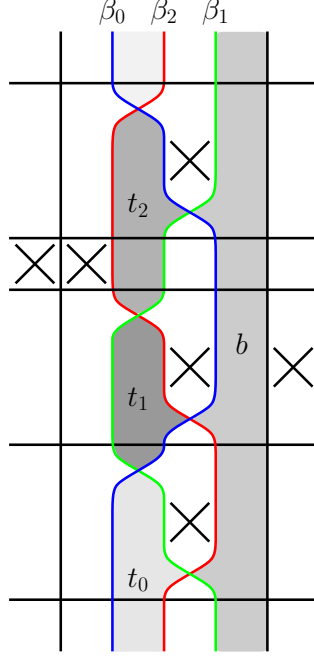


FIGURE 3.2. Combined grid diagram for L_∞, L_0 and L_1 near a point. The annulus b and the triangles t_k are shaded. The intersection points u_k are those on the right, and v_k are those on the left.

Given $\mathbf{x} \in \mathbf{S}(G_k)$ and $\mathbf{y} \in \mathbf{S}(G_{k+1})$, let $\text{Pent}_k(\mathbf{x}, \mathbf{y})$ denote the space of embedded pentagons with the following properties. First of all, $\text{Pent}_k(\mathbf{x}, \mathbf{y})$ is empty unless \mathbf{x}, \mathbf{y} coincide at exactly $n - 2$ points. An element p of $\text{Pent}_k(\mathbf{x}, \mathbf{y})$ is an embedded disk in \mathbb{T} , whose boundary consists of five arcs, each contained in horizontal or vertical circles; under the orientation induced on the boundary of p , we start at the β_k -component of \mathbf{x} , traverse the arc of a horizontal circle, meet its corresponding component of \mathbf{y} , proceed to an arc of a vertical circle, meet the corresponding component of \mathbf{x} , continue through another horizontal circle, meet the component of \mathbf{y} contained in β_{k+1} , proceed to an arc in β_{k+1} , meet the intersection point u_k of β_k and β_{k+1} , and finally, traverse an arc in β_k until we arrive back at the initial component of \mathbf{x} . Notice that all angles here are at most straight angles. The space of empty pentagons $p \in \text{Pent}_k(\mathbf{x}, \mathbf{y})$ with $\mathbf{x} \cap \text{Int}(p) = \emptyset$ is denoted $\text{Pent}_k^\circ(\mathbf{x}, \mathbf{y})$.

Similarly, we let $\text{Tri}_k(\mathbf{x}, \mathbf{y})$ denote the space of embedded triangles with the following properties. $\text{Tri}_k(\mathbf{x}, \mathbf{y})$ is empty unless \mathbf{x}, \mathbf{y} coincide at exactly $n - 1$ points. An element p of $\text{Tri}_k(\mathbf{x}, \mathbf{y})$ is an embedded disk in \mathbb{T} , whose boundary consists of three arcs, each contained in horizontal or vertical circles; under the orientation induced on the boundary of p , we start at the β_k -component of \mathbf{x} , traverse the arc of a horizontal circle, meet the component of \mathbf{y} contained in β_{k+1} , proceed to an arc in β_{k+1} , meet the intersection point v_k of β_k and β_{k+1} , and finally traverse an arc in β_k to return to the initial component of \mathbf{x} . Again, all the angles here are less than straight angles. It is clear that all triangles $p \in \text{Tri}_k(\mathbf{x}, \mathbf{y})$ satisfy $\mathbf{x} \cap \text{Int}(p) = \emptyset$.

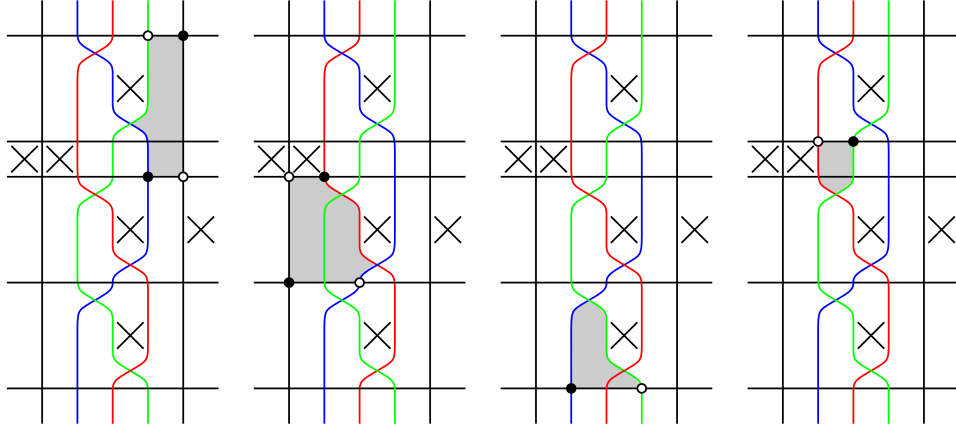


FIGURE 3.3. Two allowed pentagons in $\text{Pent}_k^\circ(\mathbf{x}, \mathbf{y})$ and two allowed triangles in $\text{Tri}_k(\mathbf{x}, \mathbf{y})$. The components of \mathbf{x} are indicated by solid points, and those of \mathbf{y} are indicated by hollow ones.

Given $\mathbf{x} \in \mathbf{S}(G_k)$, we define

$$\mathcal{P}_k(\mathbf{x}) = \sum_{\mathbf{y} \in \mathbf{S}(G_{k+1})} \sum_{\substack{p \in \text{Pent}_k^\circ(\mathbf{x}, \mathbf{y}) \\ \text{Int}(p) \cap \mathbb{X} = \emptyset}} \mathbf{y} \in C_{k+1},$$

$$\mathcal{T}_k(\mathbf{x}) = \sum_{\mathbf{y} \in \mathbf{S}(G_{k+1})} \sum_{\substack{p \in \text{Tri}_k(\mathbf{x}, \mathbf{y}) \\ \text{Int}(p) \cap \mathbb{X} = \emptyset}} \mathbf{y} \in C_{k+1},$$

and

$$f_k(\mathbf{x}) = \mathcal{P}_k(\mathbf{x}) + \mathcal{T}_k(\mathbf{x}) \in C_{k+1}.$$

Lemma 3.3. *The map f_k is a chain map. In fact, \mathcal{P}_k and \mathcal{T}_k are both chain maps.*

Proof. The proof is similar to that of Lemma 3.1 of [MOST07]. We consider domains which are obtained as the juxtaposition of a pentagon or a triangle, and a rectangle. There are a few possibilities; in particular, the polygons may be disjoint, their interiors may overlap, or they may share a common corner. If the polygons are disjoint or if their interiors overlap, the domain can be decomposed as either $r * p$ or $p * r$, and so does not contribute to $\partial_{k+1} \circ f_k + f_k \circ \partial_k$. If the polygons share a common corner, the resulting domain typically has an alternate decomposition, as shown in Figure 3.4. In all cases, the domain can be decomposed in two ways, and makes no contribution to $\partial_{k+1} \circ f_k + f_k \circ \partial_k$. Notice that there are no special cases. \square

We remark that every domain that arises as the juxtaposition of a triangle and a rectangle has exactly two decompositions, one contributing to $\partial_{k+1} \circ \mathcal{T}_k$ and one to $\mathcal{T}_k \circ \partial_k$. The analogous statement is not true for \mathcal{P}_k .

In general, when considering the composition of two maps that count polygons, we shall ignore the cases where the two polygons are disjoint or have overlapping interiors, since we can always decompose the domain as either $p_1 * p_2$ or $p_2 * p_1$ in these cases.

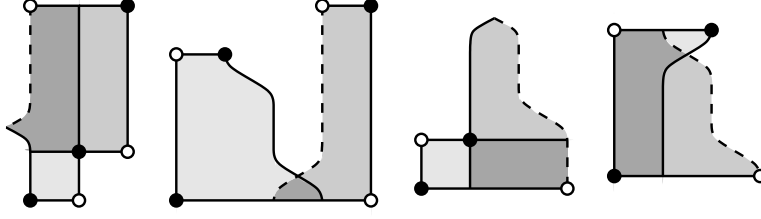


FIGURE 3.4. Two typical domains that arise as the juxtaposition of a pentagon and a rectangle, and two that arise as that of a triangle and a rectangle. The β_k curve is full while the β_{k+1} curve is dotted.

Next, we define the chain homotopies $\varphi_k: C_k \rightarrow C_{k+2}$ by counting hexagons and quadrilaterals.

Given $\mathbf{x} \in \mathbf{S}(G_k)$ and $\mathbf{y} \in \mathbf{S}(G_{k+2})$, let $\text{Hex}_k(\mathbf{x}, \mathbf{y})$ denote the space of embedded hexagons with the following properties. First of all, $\text{Hex}_k(\mathbf{x}, \mathbf{y})$ is empty unless \mathbf{x}, \mathbf{y} coincide at exactly $n - 2$ points. An element p of $\text{Hex}_k(\mathbf{x}, \mathbf{y})$ is an embedded disk in \mathcal{T} , whose boundary consists of six arcs, each contained in horizontal or vertical circles; under the orientation induced on the boundary of p , we start at the β_k -component of \mathbf{x} , traverse the arc of a horizontal circle, meet its corresponding component of \mathbf{y} , proceed to an arc of a vertical circle, meet the corresponding component of \mathbf{x} , continue through another horizontal circle, meet the component of \mathbf{y} contained in β_{k+2} , proceed to an arc in β_{k+2} , meet the intersection point u_{k+1} of β_{k+1} and β_{k+2} , traverse an arc in β_{k+1} , meet the intersection point u_k of β_k and β_{k+1} , and finally, traverse an arc in β_k until we arrive back at the initial component of \mathbf{x} . All the angles here are at most straight angles. The space of empty hexagons $p \in \text{Hex}_k(\mathbf{x}, \mathbf{y})$ with $\mathbf{x} \cap \text{Int}(p) = \emptyset$ is denoted $\text{Hex}_k^\circ(\mathbf{x}, \mathbf{y})$.

Similarly, we let $\text{Quad}_k(\mathbf{x}, \mathbf{y})$ denote the space of embedded quadrilaterals with the following properties. $\text{Quad}_k(\mathbf{x}, \mathbf{y})$ is empty unless \mathbf{x}, \mathbf{y} coincide at exactly $n - 1$ points. An element p of $\text{Quad}_k(\mathbf{x}, \mathbf{y})$ is an embedded disk in \mathcal{T} , whose boundary consists of four arcs, each contained in horizontal or vertical circles; under the orientation induced on the boundary of p , we start at the β_k -component of \mathbf{x} , traverse the arc of a horizontal circle, meet the component of \mathbf{y} contained in β_{k+2} , proceed to an arc in β_{k+2} , meet the intersection point u_{k+1} of β_{k+1} and β_{k+2} , proceed to an arc in β_{k+1} , meet the intersection point v_k of β_k with β_{k+1} , and finally traverse an arc in β_k to return to the initial component of \mathbf{x} . All the angles here are at most straight angles. It is clear that all quadrilaterals $p \in \text{Tri}_k(\mathbf{x}, \mathbf{y})$ satisfy $\mathbf{x} \cap \text{Int}(p) = \emptyset$.

Given $\mathbf{x} \in \mathbf{S}(G_k)$, we define

$$\begin{aligned} \mathcal{H}_k(\mathbf{x}) &= \sum_{\mathbf{y} \in \mathbf{S}(G_{k+1})} \sum_{\substack{p \in \text{Hex}_k^\circ(\mathbf{x}, \mathbf{y}) \\ \text{Int}(p) \cap \mathbb{X} = \emptyset}} \mathbf{y} \in C_{k+2}, \\ \mathcal{Q}_k(\mathbf{x}) &= \sum_{\mathbf{y} \in \mathbf{S}(G_{k+1})} \sum_{\substack{p \in \text{Quad}_k(\mathbf{x}, \mathbf{y}) \\ \text{Int}(p) \cap \mathbb{X} = \emptyset}} \mathbf{y} \in C_{k+2}, \end{aligned}$$

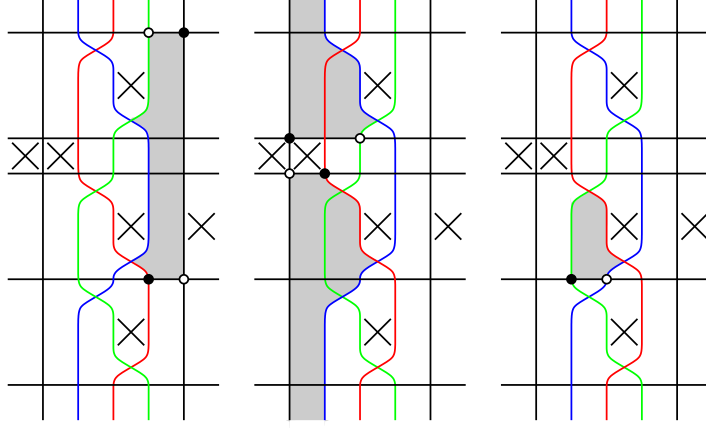


FIGURE 3.5. Two allowed hexagons in $\text{Hex}_k^\circ(\mathbf{x}, \mathbf{y})$ and an allowed quadrilateral in $\text{Quad}_k(\mathbf{x}, \mathbf{y})$.

and

$$\varphi_k(\mathbf{x}) = \mathcal{H}_k(\mathbf{x}) + \mathcal{Q}_k(\mathbf{x}) \in C_{k+2}.$$

We say that a domain p is a *left domain* if $\text{Int}(p) \cap \text{Int}(b) = \emptyset$, and a *right domain* if $\text{Int}(p) \cap \text{Int}(b) \neq \emptyset$.

Lemma 3.4. *The maps f_k and φ_k satisfy Condition (1) of Lemma 3.2.*

Proof. Juxtaposing a triangle and a pentagon appearing in $\mathcal{P}_{k+1} \circ \mathcal{T}_k$, we generically obtain a composite domain that admits a unique alternative decomposition as a quadrilateral and a square, appearing in either $\partial_{k+2} \circ \mathcal{Q}_k$ or $\mathcal{Q}_k \circ \partial_k$. Juxtaposing two pentagons appearing in $\mathcal{P}_{k+1} \circ \mathcal{P}_k$, we generically obtain a composite domain that admits a unique alternative decomposition as a hexagon and a square, appearing in either $\partial_{k+2} \circ \mathcal{H}_k$ or $\mathcal{H}_k \circ \partial_k$, except for one special case, which is described in (2) below.

There are two special cases: We consider domains p , arising from the juxtaposition of

- (1) a pentagon and a triangle appearing in $\mathcal{T}_{k+1} \circ \mathcal{P}_k$. The domain p can only be alternatively decomposed as the triangle t_{k+2} and a pentagon, bounded by β_k , a horizontal arc, a vertical arc, another horizontal arc and β_{k+2} , in its induced orientation. The pentagon is in the opposite orientation as one that would be counted in the map f_{k+2} , and its boundary meets only the intersection point v_{k+2} ; such a pentagon is not counted in any map. The triangle t_{k+2} is not counted in any map either. Therefore, p is counted exactly once in $f_{k+1} \circ f_k + \partial_{k+2} \circ \varphi_k + \varphi_k \circ \partial_k$. However, we can replace t_{k+2} with the triangle t_k , and obtain a corresponding domain p' that also connects \mathbf{x} to \mathbf{y} . The new domain p' admits a unique alternative decomposition as a quadrilateral and a square, counted in $\partial_{k+2} \circ \mathcal{Q}_k$. See Figure 3.6 (1).
- (2) two triangles appearing in $\mathcal{T}_{k+1} \circ \mathcal{T}_k$. The domain p can only be alternatively decomposed as the triangle t_{k+1} and another triangle, bounded by

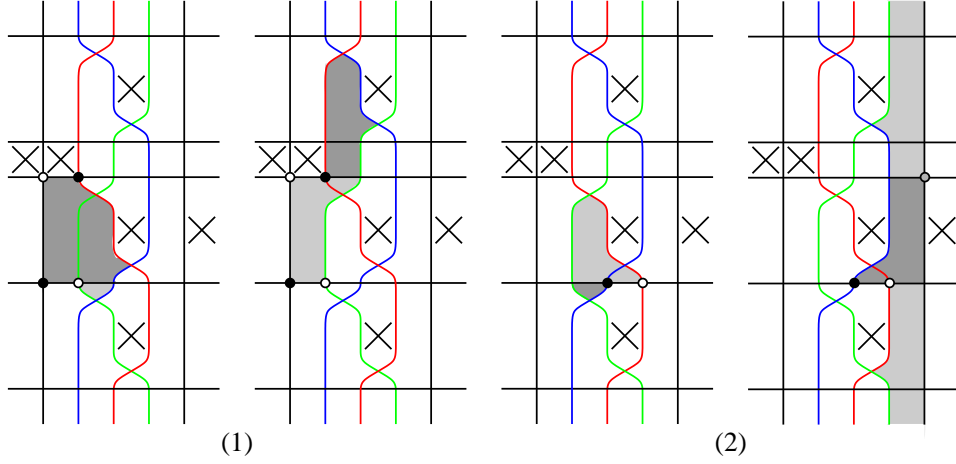


FIGURE 3.6. Two special cases. In each case, there are two domains p and p' , each counted exactly once in $f_{k+1} \circ f_k + \partial_{k+2} \circ \varphi_k + \varphi_k \circ \partial_k$.

β_k, β_{k+2} and a horizontal arc, in its induced orientation. Since neither triangle is counted in any of the maps f_k or φ_k , p is counted exactly once in $f_{k+1} \circ f_k + \partial_{k+2} \circ \varphi_k + \varphi_k \circ \partial_k$. However, we can replace t_{k+1} with the annulus b , and obtain a corresponding domain p' that also connects \mathbf{x} to \mathbf{y} . The situation is similar to the special case in the proof of Lemma 3.1 of [MOST07]. Depending on the initial point \mathbf{x} , the new domain p' admits a unique alternative decomposition as two pentagons or as a hexagon and a square, counted either in $\mathcal{P}_{k+1} \circ \mathcal{P}_k$, in $\partial_{k+2} \circ \mathcal{H}_k$, or in $\mathcal{H}_k \circ \partial_k$. See Figure 3.6 (2).

Finally, there are no other terms in $\partial_{k+2} \circ \mathcal{Q}_k$ or $\mathcal{Q}_k \circ \partial_k$, and the remaining terms in $\partial_{k+2} \circ \mathcal{H}_k$ cancel with terms in $\mathcal{H}_k \circ \partial_k$. Table 3.1 summarizes how the terms cancel each other. \square

We now define the chain homotopy $\psi_k: C_k \rightarrow C_k$ by counting heptagons.

Given $\mathbf{x} \in \mathbf{S}(G_0)$ and $\mathbf{y} \in \mathbf{S}(G_2)$, let $\text{Hept}_k(\mathbf{x}, \mathbf{y})$ denote the space of embedded heptagons. First of all, $\text{Hept}_k(\mathbf{x}, \mathbf{y})$ is empty unless \mathbf{x}, \mathbf{y} coincide at exactly $n - 2$ points. An element p of $\text{Hept}_k(\mathbf{x}, \mathbf{y})$ is an embedded disk in \mathbb{T} , whose boundary consists of seven arcs, each contained in horizontal or vertical circles; under the orientation induced on the boundary of p , we start at the β_k -component of \mathbf{x} , traverse the arc of a horizontal circle, meet its corresponding component of \mathbf{y} , proceed to an arc of a vertical circle, meet the corresponding component of \mathbf{x} , continue through another horizontal circle, meet the component of \mathbf{y} contained in β_k , proceed to an arc in β_k , meet the intersection point u_{k+2} of β_k and β_{k+2} , proceed to an arc in β_{k+2} , meet the intersection point u_{k+1} of β_{k+1} and β_{k+2} , traverse an arc in β_{k+1} , meet the intersection point u_k of β_k and β_{k+1} , and finally, traverse an arc in β_k until we arrive back at the initial component of \mathbf{x} . All the angles here are again at most straight angles. The space of empty heptagons $p \in \text{Hept}_k(\mathbf{x}, \mathbf{y})$ with $\mathbf{x} \cap \text{Int}(p) = \emptyset$ is denoted $\text{Hept}_k^\circ(\mathbf{x}, \mathbf{y})$.

Term in		Position	Cancels with Term in	Sp. Case
$f_{k+1} \circ f_k$	$\mathcal{P}_{k+1} \circ \mathcal{P}_k$	left, right ($\not\supset b$)	$\partial_{k+2} \circ \mathcal{H}_k$ or $\mathcal{H}_k \circ \partial_k$	
		right ($\supset b$)	$\mathcal{T}_{k+1} \circ \mathcal{T}_k$	(2)
	$\mathcal{T}_{k+1} \circ \mathcal{P}_k$	left	$\partial_{k+2} \circ \mathcal{Q}_k$	(1)
		right	$\mathcal{Q}_k \circ \partial_k$	
	$\mathcal{T}_{k+1} \circ \mathcal{T}_k$	left	$\mathcal{P}_{k+1} \circ \mathcal{P}_k, \partial_{k+2} \circ \mathcal{H}_k$ or $\mathcal{H}_k \circ \partial_k$	(2)
$\partial_{k+2} \circ \varphi_k$	$\partial_{k+2} \circ \mathcal{H}_k$	left, right ($\not\supset b$)	$\mathcal{P}_k \circ \mathcal{P}_k$ or $\mathcal{H}_k \circ \partial_k$	
		right ($\supset b$)	$\mathcal{T}_{k+1} \circ \mathcal{T}_k$	(2)
	$\partial_{k+2} \circ \mathcal{Q}_k$	left	$\mathcal{T}_{k+1} \circ \mathcal{P}_k$	(1)
		right	$\mathcal{P}_{k+1} \circ \mathcal{T}_k$	
$\varphi_k \circ \partial_k$	$\mathcal{H}_k \circ \partial_k$	left, right ($\not\supset b$)	$\mathcal{P}_{k+1} \circ \mathcal{P}_k$ or $\partial_{k+2} \circ \mathcal{H}_k$	
		right ($\supset b$)	$\mathcal{T}_{k+1} \circ \mathcal{T}_k$	(2)
	$\mathcal{Q}_k \circ \partial_k$	left	$\mathcal{P}_{k+1} \circ \mathcal{T}_k$	

TABLE 3.1. This table shows how the terms cancel each other in Lemma 3.4. A right domain is indicated as “($\supset b$)” if $\text{Int}(p) \supset \text{Int}(b)$, and “($\not\supset b$)” otherwise. The special cases are shown in Figure 3.6.

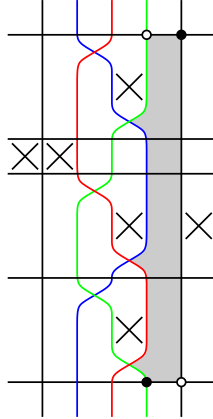


FIGURE 3.7. An allowed heptagon in $\text{Hept}_k^o(\mathbf{x}, \mathbf{y})$.

Given $\mathbf{x} \in \mathbf{S}(G_k)$, we define

$$\psi_k(\mathbf{x}) = \mathcal{K}_k(\mathbf{x}) = \sum_{\mathbf{y} \in \mathbf{S}(G_{k+1})} \sum_{\substack{p \in \text{Hept}_k^o(\mathbf{x}, \mathbf{y}) \\ \text{Int}(p) \cap \mathbb{X} = \emptyset}} \mathbf{y} \in C_k.$$

Lemma 3.5. *We have*

$$\varphi_{k+1} \circ f_k + f_{k+2} \circ \varphi_k + \partial_k \circ \psi_k + \psi_k \circ \partial_k = \text{Id},$$

so that the maps f_k and φ_k satisfy Condition (2) of Lemma 3.2.

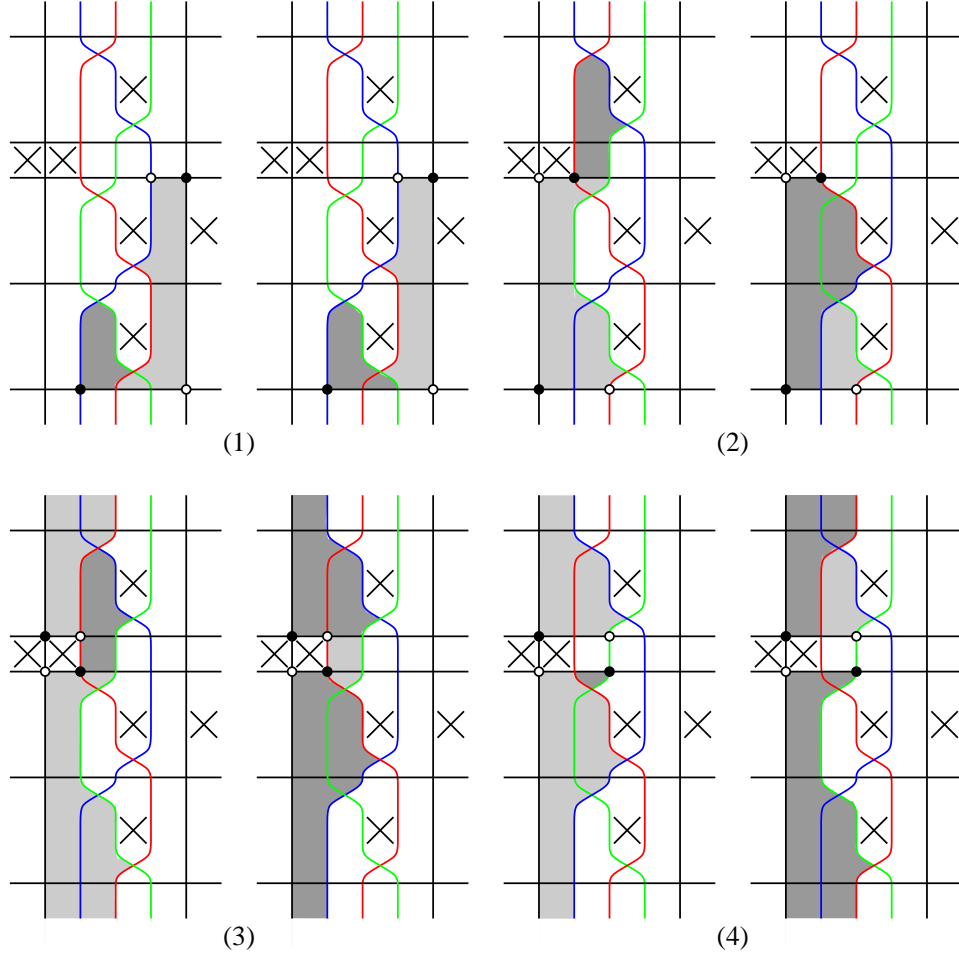


FIGURE 3.8. The four cases when juxtaposing a triangle and a hexagon, or a pentagon and a quadrilateral. All terms that arise cancel out with each other.

Proof. First, we see that juxtaposing either a triangle and a hexagon, or a pentagon and a quadrilateral, does not contribute to $\varphi_{k+1} \circ f_k + f_{k+2} \circ \varphi_k$. There are exactly four cases: We consider domains p formed by juxtaposing

- (1) a quadrilateral and a pentagon appearing in $\mathcal{P}_{k+2} \circ \mathcal{Q}_k$, such that p is a right domain. In this case, p admits a unique alternative decomposition as a triangle and a hexagon appearing in $\mathcal{H}_{k+1} \circ \mathcal{T}_k$. See Figure 3.8 (1);
- (2) a quadrilateral and a pentagon appearing in $\mathcal{P}_{k+2} \circ \mathcal{Q}_k$, such that p is a left domain with height less than n . Only this decomposition of p is counted. However, we can replace the triangle t_k inside p by the triangle t_{k+2} , and obtain a corresponding domain p' that can be uniquely decomposed as a pentagon and a quadrilateral appearing in $\mathcal{Q}_{k+1} \circ \mathcal{P}_k$. See Figure 3.8 (2);
- (3) a quadrilateral and a pentagon appearing in $\mathcal{P}_{k+2} \circ \mathcal{Q}_k$, such that p is a right domain with height n . This is in fact only possible when $k = 2$. Only

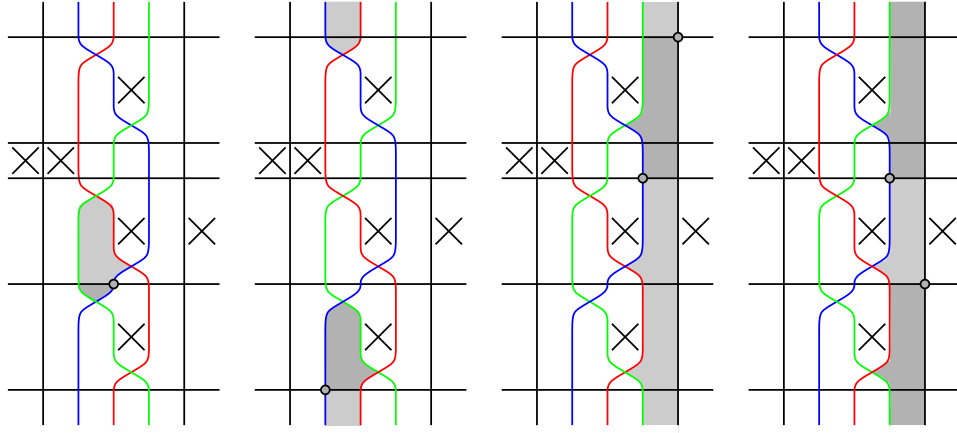


FIGURE 3.9. Decomposing the identity map.

this decomposition of p is counted. However, p contains the triangles t_k and t_{k+1} ; we can replace t_{k+1} by the triangle t_{k+2} , and obtain a corresponding domain p' that can be uniquely decomposed as a hexagon and a triangle appearing in $\mathcal{T}_{k+2} \circ \mathcal{H}_k$. See Figure 3.8 (3).

The astute reader may find it strange that in this particular case, in p the triangle t_k is “attached” to the top of the rest of the domain, whereas in p' it is “attached” to the bottom. One way to convince oneself of the validity of the procedure of obtaining p' from p , is to think of it as first replacing t_k by t_{k+2} , and then replacing t_{k+1} by t_k ;

- (4) a triangle and a hexagon appearing in $\mathcal{H}_{k+1} \circ \mathcal{T}_k$, such that p is a left domain. This is only possible when $k = 1$. Only this decomposition of p is counted. However, we can replace the triangle t_k inside p by the triangle t_{k+2} , and obtain a corresponding domain p' that can be uniquely decomposed as a pentagon and a quadrilateral appearing in $\mathcal{Q}_{k+1} \circ \mathcal{P}_k$. See Figure 3.8 (4).

Juxtaposing a pentagon and a hexagon appearing in $\mathcal{H}_{k+1} \circ \mathcal{P}_k$ or $\mathcal{P}_{k+2} \circ \mathcal{H}_k$, we generically obtain a composite domain that admits a unique alternative decomposition as a heptagon and a square, appearing in $\partial_k \circ \mathcal{K}_k$ or $\mathcal{K}_k \circ \partial_k$, except for one special case discussed below.

Depending on the initial point \mathbf{x} , there exists exactly one domain p connecting \mathbf{x} to itself that admits a unique decomposition, either as a triangle and a quadrilateral in $\mathcal{Q}_{k+1} \circ \mathcal{T}_k$ (in which case p is the triangle t_{k+1}), as a quadrilateral and a triangle in $\mathcal{T}_{k+2} \circ \mathcal{Q}_k$ (p is the triangle t_k), or as a pentagon and a hexagon appearing in $\mathcal{H}_{k+1} \circ \mathcal{P}_k$ or $\mathcal{P}_{k+2} \circ \mathcal{H}_k$ (p is the annulus b). Of course, in this case, the identity map is counted once. See Figure 3.9.

Finally, the remaining terms in $\partial_k \circ \mathcal{K}_k$ cancel with terms in $\mathcal{K}_k \circ \partial_k$. Table 3.2 summarizes how the terms above cancel each other. \square

The proof of Proposition 3.1 is completed by combining Lemmas 3.2, 3.3, 3.4 and 3.5.

Term in		Position	Cancels with Term in	Sp. Case
$\varphi_{k+1} \circ f_k$	$\mathcal{H}_{k+1} \circ \mathcal{P}_k$	right ($\neq b$)	$\partial_k \circ \mathcal{K}_k$ or $\mathcal{K}_k \circ \partial_k$	
		right ($= b$)	Id	
	$\mathcal{Q}_{k+1} \circ \mathcal{P}_k$	left (ht. $< n-1$)	$\mathcal{P}_{k+2} \circ \mathcal{Q}_k$	(2)
		left (ht. $= n-1$)	$\mathcal{H}_{k+1} \circ \mathcal{T}_k$	(4)
	$\mathcal{H}_{k+1} \circ \mathcal{T}_k$	left	$\mathcal{Q}_{k+1} \circ \mathcal{P}_k$	(4)
		right	$\mathcal{P}_{k+2} \circ \mathcal{Q}_k$	(1)
	$\mathcal{Q}_{k+1} \circ \mathcal{T}_k$	left	Id	
$f_{k+2} \circ \varphi_k$	$\mathcal{P}_{k+2} \circ \mathcal{H}_k$	right ($\neq b$)	$\partial_k \circ \mathcal{K}_k$ or $\mathcal{K}_k \circ \partial_k$	
		right ($= b$)	Id	
	$\mathcal{T}_{k+2} \circ \mathcal{H}_k$	left	$\mathcal{P}_{k+2} \circ \mathcal{Q}_k$	(3)
	$\mathcal{P}_{k+2} \circ \mathcal{Q}_k$	left (ht. $< n$)	$\mathcal{Q}_{k+1} \circ \mathcal{P}_k$	(2)
		left (ht. $= n$)	$\mathcal{T}_{k+1} \circ \mathcal{H}_k$	(3)
		right	$\mathcal{H}_{k+1} \circ \mathcal{T}_k$	(1)
	$\mathcal{T}_{k+2} \circ \mathcal{Q}_k$	left	Id	
$\partial_k \circ \psi_k$	$\partial_k \circ \mathcal{K}_k$	right	$\mathcal{H}_{k+1} \circ \mathcal{P}_k, \mathcal{P}_{k+2} \circ \mathcal{H}_k$ or $\mathcal{K}_k \circ \partial_k$	
$\psi_k \circ \partial_k$	$\mathcal{K}_k \circ \partial_k$	right	$\mathcal{H}_{k+1} \circ \mathcal{P}_k, \mathcal{P}_{k+2} \circ \mathcal{H}_k$ or $\partial_k \circ \mathcal{K}_k$	
Id		N/A	$\mathcal{H}_{k+1} \circ \mathcal{P}_k, \mathcal{P}_{k+2} \circ \mathcal{H}_k,$ $\mathcal{Q}_{k+1} \circ \mathcal{T}_k$ or $\mathcal{T}_{k+2} \circ \mathcal{Q}_k$	

TABLE 3.2. This table shows how the terms cancel each other in Lemma 3.5. The special cases are shown in Figure 3.8.

4. SIGNS

In [MOST07], sign refinements are given to extend the definition of combinatorial knot Floer homology to one with coefficients in \mathbb{Z} . In this section, we shall likewise assign sign refinements to our maps, to prove the analogous statement of Proposition 3.1 with coefficients in \mathbb{Z} .

Given a grid diagram, we denote by Rect° the union of $\text{Rect}^\circ(\mathbf{x}, \mathbf{y})$ for all \mathbf{x}, \mathbf{y} . We follow [MOST07] and adopt the following definition:

Definition 4.1. A *true sign assignment*, or simply a *sign assignment*, is a function

$$\mathcal{S}: \text{Rect}^\circ \rightarrow \{\pm 1\}$$

with the following properties:

- (1) For any four distinct $r_1, r_2, r'_1, r'_2 \in \text{Rect}^\circ$ with $r_1 * r_2 = r'_1 * r'_2$, we have

$$\mathcal{S}(r_1) \cdot \mathcal{S}(r_2) = -\mathcal{S}(r'_1) \cdot \mathcal{S}(r'_2);$$

- (2) For $r_1, r_2 \in \text{Rect}^\circ$ such that $r_1 * r_2$ is a vertical annulus, we have

$$\mathcal{S}(r_1) \cdot \mathcal{S}(r_2) = -1;$$

- (3) For $r_1, r_2 \in \text{Rect}^\circ$ such that $r_1 * r_2$ is a horizontal annulus, we have

$$\mathcal{S}(r_1) \cdot \mathcal{S}(r_2) = +1.$$

Theorem 4.2 (Manolescu–Ozsváth–Szabó–Thurston). *There exists a sign assignment as defined in Definition 4.1. Moreover, this sign assignment is essentially unique: If \mathcal{S}_1 and \mathcal{S}_2 are two sign assignments, then there is a function $g: \mathbf{S}(G) \rightarrow \{\pm 1\}$ so that for all $r \in \text{Rect}^\circ(\mathbf{x}, \mathbf{y})$, $\mathcal{S}_2(r) = g(\mathbf{x}) \cdot g(\mathbf{y}) \cdot \mathcal{S}_1(r)$.*

We remark here that in the construction of a sign assignment in [MOST07], the sign of a rectangle does not depend on the positions of the O 's and X 's of the diagram. We can view each generator \mathbf{x} as a permutation $\sigma_{\mathbf{x}}$; If the component of \mathbf{x} on the i -th horizontal circle lies on the $s(i)$ -th vertical circle, then we let $\sigma_{\mathbf{x}}$ be $(s(1) s(2) \dots s(n))$. Then the sign of a rectangle in $\text{Rect}^\circ(\mathbf{x}, \mathbf{y})$ depends only on $\sigma_{\mathbf{x}}$ and $\sigma_{\mathbf{y}}$.

The sign assignment from Theorem 4.2 is then used in [MOST07] to construct a chain complex over \mathbb{Z} as follows. The complex $C(G)$ is the free \mathbb{Z} -module generated by elements of $\mathbf{S}(G)$; fixing a sign assignment \mathcal{S} , the complex $C(G)$ is endowed with the endomorphism $\partial_{\mathcal{S}}: C(G) \rightarrow C(G)$, defined by

$$\partial_{\mathcal{S}}(\mathbf{x}) = \sum_{\mathbf{y} \in \mathbf{S}(G)} \sum_{\substack{r \in \text{Rect}^\circ(\mathbf{x}, \mathbf{y}) \\ \text{Int}(r) \cap \mathbb{X} = \emptyset}} \mathcal{S}(r) \cdot \mathbf{y} \in C(G).$$

One can then see that $(C(G), \partial_{\mathcal{S}})$ is a chain complex. Indeed, the terms in $\partial_{\mathcal{S}} \circ \partial_{\mathcal{S}}(\mathbf{x})$ can be paired off as before, by the axioms defining \mathcal{S} . Moreover, given \mathcal{S}_1 and \mathcal{S}_2 , the map $\Phi: (C(G), \partial_{\mathcal{S}_1}) \rightarrow (C(G), \partial_{\mathcal{S}_2})$, defined by

$$\Phi(\mathbf{x}) = g(\mathbf{x}) \cdot \mathbf{x},$$

gives an isomorphism of the two chain complexes. Again, one can take the homology of the chain complex $(C(G), \partial_{\mathcal{S}})$, and define

$$\widehat{\text{HK}}(G) = H_*(C(G), \partial_{\mathcal{S}}).$$

It is shown in [MOST07] that

$$\widehat{\text{HK}}(G) \cong \widehat{\text{HK}}(G) \otimes V^{n-\ell}$$

for some \mathbb{Z} -module $\widehat{\text{HK}}(G)$ that is a link invariant, where V is a rank-2 free module over \mathbb{Z} , spanned by one generator in bigrading $(-1, -1)$ and another in bigrading $(0, 0)$. The link invariant $\widehat{\text{HK}}(G)$, also denoted by $\widehat{\text{HFK}}(L)$, is shown in [Sar11] to be isomorphic to $\widehat{\text{HFK}}(L, \mathfrak{o})$ for some *orientation system* \mathfrak{o} of the link L .

We are now ready to turn to the proof of the analogous statement of Proposition 3.1, with signs.

Proposition 4.3. *Let the base ring be \mathbb{Z} . There exists an exact triangle*

$$\dots \rightarrow \widehat{\text{HK}}(G_0) \rightarrow \widehat{\text{HK}}(G_1) \rightarrow \widehat{\text{HK}}(G_2) \rightarrow \dots$$

Our proof is reminiscent of that in Section 4 of [MOST07]. We adopt the strategy from Section 3; to do so, we must specify the signs used in defining our various chain maps and chain homotopies, and check that they indeed satisfy the following modified version of Lemma 3.2:

Lemma 4.4. *Let $\{(C_k, \partial_k)\}_{k \in \mathbb{Z}/3\mathbb{Z}}$ be a collection of chain complexes over \mathbb{Z} , and let $\{f_k: C_k \rightarrow C_{k+1}\}_{k \in \mathbb{Z}/3\mathbb{Z}}$ be a collection of anti-chain maps such that the following conditions are satisfied for each k :*

- (1) The composite $f_{k+1} \circ f_k : C_k \rightarrow C_{k+2}$ is chain-homotopic to zero, by a chain homotopy $\varphi_k : C_k \rightarrow C_{k+2}$:

$$f_{k+1} \circ f_k + \partial_{k+2} \circ \varphi_k + \varphi_k \circ \partial_k = 0;$$

- (2) The map $\varphi_{k+1} \circ f_k + f_{k+2} \circ \varphi_k : C_k \rightarrow C_k$ is a quasi-isomorphism. (In particular, if there exists a chain homotopy $\psi_k : C_k \rightarrow C_k$ such that

$$\varphi_{k+1} \circ f_k + f_{k+2} \circ \varphi_k + \partial_k \circ \psi_k + \psi_k \circ \partial_k = \text{Id},$$

then this condition is satisfied.)

Then the sequence

$$\cdots \rightarrow H_*(C_k) \xrightarrow{(f_k)_*} H_*(C_{k+1}) \xrightarrow{(f_{k+1})_*} H_*(C_{k+2}) \rightarrow \cdots$$

is exact.

We begin by considering pentagons. First, we define the notion of a *corresponding generator*. For each $\mathbf{x} \in C_k$, there exist exactly one $\mathbf{x}' \in C_{k+1}$ and one $\mathbf{x}'' \in C_{k+2}$ that are canonically closest to \mathbf{x} ; we require that \mathbf{x}, \mathbf{x}' and \mathbf{x}'' coincide everywhere except on the β -curves, and \mathbf{x}' and \mathbf{x}'' are obtained from \mathbf{x} by sliding the β_k -component horizontally to the β_{k+1} and β_{k+2} curves respectively. We define the maps $c_k^+ : C_k \rightarrow C_{k+1}$ and $c_k^- : C_k \rightarrow C_{k+2}$ by

$$\begin{aligned} c_k^+(\mathbf{x}) &= \mathbf{x}', \\ c_k^-(\mathbf{x}) &= \mathbf{x}''. \end{aligned}$$

We can now define the straightening maps $d_k^{\mathcal{P}} : \text{Pent}_k^{\circ}(\mathbf{x}, \mathbf{y}) \rightarrow \text{Rect}_k^{\circ}(\mathbf{x}, c_k^-(\mathbf{y}))$ and $e_k^{\mathcal{P}} : \text{Pent}_k^{\circ}(\mathbf{x}, \mathbf{y}) \rightarrow \text{Rect}_{k+1}^{\circ}(c_k^+(\mathbf{x}), \mathbf{y})$ as follows. Given $p \in \text{Pent}_k^{\circ}(\mathbf{x}, \mathbf{y})$, we obtain $d_k^{\mathcal{P}}(p)$ by sliding the β_{k+1} -component of \mathbf{y} back to the β_k -curve, thereby post-composing p with a triangle; similarly, we obtain $e_k^{\mathcal{P}}(p)$ by sliding the β_k -component of \mathbf{x} to the β_{k+1} -curve, thereby pre-composing p with another triangle. Notice that by the remark after Theorem 4.2, we have

$$\mathcal{S}(d_k^{\mathcal{P}}(p)) = \mathcal{S}(e_k^{\mathcal{P}}(p)).$$

We now define

$$\mathcal{P}_k(\mathbf{x}) = \sum_{\mathbf{y} \in \mathbf{S}(G_{k+1})} \sum_{\substack{p \in \text{Pent}_k^{\circ}(\mathbf{x}, \mathbf{y}) \\ \text{Int}(p) \cap \mathbb{X} = \emptyset}} \epsilon_k^{\mathcal{P}}(p) \cdot \mathbf{y} \in C_{k+1},$$

where

$$\epsilon_k^{\mathcal{P}}(p) = \begin{cases} \mathcal{S}(d_k^{\mathcal{P}}(p)) & \text{if } p \text{ is a left pentagon,} \\ -\mathcal{S}(d_k^{\mathcal{P}}(p)) & \text{if } p \text{ is a right pentagon.} \end{cases}$$

Turning to triangles, we again view generators as permutations. The signature $\text{sgn}(\mathbf{x})$ of a generator \mathbf{x} is defined to be the signature $\text{sgn}(\sigma_{\mathbf{x}})$ of the corresponding permutation. Then we define

$$\mathcal{T}_k(\mathbf{x}) = \sum_{\mathbf{y} \in \mathbf{S}(G_{k+1})} \sum_{\substack{p \in \text{Tri}_k(\mathbf{x}, \mathbf{y}) \\ \text{Int}(p) \cap \mathbb{X} = \emptyset}} \epsilon_k^{\mathcal{T}}(p) \cdot \mathbf{y} \in C_{k+1},$$

where

$$\epsilon_k^{\mathcal{T}}(p) = \text{sgn}(\mathbf{x}).$$

Finally, we define

$$f_k(\mathbf{x}) = \mathcal{P}_k(\mathbf{x}) + \mathcal{T}_k(\mathbf{x}) \in C_{k+1}.$$

Lemma 4.5. *The map f_k is an anti-chain map. In fact, \mathcal{P}_k and \mathcal{T}_k are both anti-chain maps.*

Proof. The proof follows from the proof of Lemma 3.3. We first consider the juxtaposition of a pentagon and a rectangle. If the two polygons are disjoint or have overlapping interiors, then the domain can be decomposed as either $r * p$ or $p' * r'$; then by Property (1) of Definition 4.1, $\mathcal{S}(r) \cdot \mathcal{S}(d_k^{\mathcal{P}}(p)) = -\mathcal{S}(d_k^{\mathcal{P}}(p')) \cdot \mathcal{S}(r')$, and consequently $\mathcal{S}(r) \cdot \epsilon_k^{\mathcal{P}}(p) = -\epsilon_k^{\mathcal{P}}(p') \cdot \mathcal{S}(r')$. If the two polygons share a corner, then the domain can be decomposed in two ways; straightening the pentagons (with either $d_k^{\mathcal{P}}$ or $e_k^{\mathcal{P}}$) and using Property (1) of Definition 4.1, we again see that the terms cancel.

Consider now the juxtaposition of a triangle p and a rectangle r . Notice first that the differential ∂ always changes the signature of a generator; this means that $\mathcal{S}(r) \cdot \epsilon_k^{\mathcal{T}}(p) = -\epsilon_k^{\mathcal{T}}(p') \cdot \mathcal{S}(r')$. We remarked immediately after Lemma 3.3 that such a domain can always be decomposed in two ways, one contributing to $\partial_{k+1} \circ \mathcal{T}_k$, and one to $\mathcal{T}_k \circ \partial_k$; moreover, the two rectangles involved correspond to the same permutation, and so in fact have the same sign. \square

We similarly define the straightening maps $d_k^{\mathcal{H}}: \text{Hex}_k^{\circ}(\mathbf{x}, \mathbf{y}) \rightarrow \text{Rect}_k^{\circ}(\mathbf{x}, c_k^+(\mathbf{y}))$ and $e_k^{\mathcal{H}}: \text{Hex}_k^{\circ}(\mathbf{x}, \mathbf{y}) \rightarrow \text{Rect}_{k+2}^{\circ}(c_k^-(\mathbf{x}), \mathbf{y})$ by sliding the appropriate component, and again notice that $\mathcal{S}(d_k^{\mathcal{H}}(p)) = \mathcal{S}(e_k^{\mathcal{H}}(p))$. We define

$$\mathcal{H}_k(\mathbf{x}) = \sum_{\mathbf{y} \in \mathbf{S}(G_{k+2})} \sum_{\substack{p \in \text{Hex}_k^{\circ}(\mathbf{x}, \mathbf{y}) \\ \text{Int}(p) \cap \mathbb{X} = \emptyset}} \epsilon_k^{\mathcal{H}}(p) \cdot \mathbf{y} \in C_{k+2},$$

where

$$\epsilon_k^{\mathcal{H}}(p) = \mathcal{S}(d_k^{\mathcal{H}}(p)).$$

For quadrilaterals,

$$\mathcal{Q}_k(\mathbf{x}) = \sum_{\mathbf{y} \in \mathbf{S}(G_{k+2})} \sum_{\substack{p \in \text{Quad}_k^{\circ}(\mathbf{x}, \mathbf{y}) \\ \text{Int}(p) \cap \mathbb{X} = \emptyset}} \epsilon_k^{\mathcal{Q}}(p) \cdot \mathbf{y} \in C_{k+2},$$

where

$$\epsilon_k^{\mathcal{Q}}(p) = \text{sgn}(\mathbf{x}).$$

Lemma 4.6. *The maps f_k and φ_k satisfy Condition (1) of Lemma 4.4.*

Proof. Again the proof follows from that of Lemma 3.4. We say that a domain p is *rectangle-like* if it is an allowed rectangle, pentagon, hexagon or heptagon, and we write $p \in \text{RL}$; we say that it is *triangle-like* if it is an allowed triangle or quadrilateral, and we write $p \in \text{TL}$. We call a domain p *Type I* if $p \in \text{RL} * \text{RL}$; *Type II* if $p \in \text{RL} * \text{TL}$, *Type III* if $p \in \text{TL} * \text{RL}$, and *Type IV* if $p \in \text{TL} * \text{TL}$. Refer to Table 3.1. Typically, a domain can be decomposed in two ways; usually, it fits into one of these cases:

- (1) Both decompositions are Type I. In this case, we see that the terms cancel out by straightening the polygons and applying Property (1) of Definition 4.1;
- (2) One decomposition is Type II, and one is Type III. The domain is a left domain. In this case, the terms cancel out because the two rectangle-like polygons have the same sign, but the two triangle-like polygons have opposite signs;

- (3) Both decompositions are Type III. The domain is a right domain. In this case, the two triangle-like polygons have the same sign. However, the two rectangle-like polygons are both right domains, and one is a rectangle or hexagon, and the other a pentagon. Since right pentagons have opposite signs as the straightened rectangles, the two rectangle-like polygons are of opposite signs.

The only special cases are those that involve two different domains, which are exactly the special cases in Lemma 3.4.

- (1) In this case, the rectangle and the pentagon have the same sign, but the triangle and the quadrilateral have opposite signs;
- (2) In one domain, the two triangles have the same sign, and so their composite is positive; in the other domain, the composite of the straightened rectangles is a vertical annulus, and so is negative by Property (2) of Definition 4.1.

Since there are no other cases, our proof is complete. \square

Now for heptagons, there is only one straightening map $d_k^K: \text{Hept}_k^\circ(\mathbf{x}, \mathbf{y}) \rightarrow \text{Rect}_k^\circ(\mathbf{x}, \mathbf{y})$. Seeing that the only allowed heptagons are right heptagons, we define

$$\mathcal{K}_k(\mathbf{x}) = \sum_{\mathbf{y} \in \mathbf{S}(G_{k+2})} \sum_{\substack{p \in \text{Hept}_k^\circ(\mathbf{x}, \mathbf{y}) \\ \text{Int}(p) \cap \mathbb{X} = \emptyset}} \epsilon_k^K(p) \cdot \mathbf{y} \in C_k,$$

where

$$\epsilon_k^K(p) = -\mathcal{S}(d_k^K(p)).$$

Lemma 4.7. *We have*

$$\varphi_{k+1} \circ f_k + f_{k+2} \circ \varphi_k + \partial_k \circ \psi_k + \psi_k \circ \partial_k = \text{Id},$$

so that the maps f_k and φ_k satisfy Condition (2) of Lemma 4.4.

Proof. The typical cases are as in the proof of Lemma 4.6. We check the special cases in Lemma 3.5.

- (1) This is actually a typical case; the two decompositions of the domain are both Type III;
- (2) In this case, the pentagons have the same sign, but the quadrilaterals have opposite signs;
- (3) In this case, the pentagon and the hexagon have the same sign, but the triangle and the quadrilateral have opposite signs;
- (4) Also in this case, the pentagon and the hexagon have the same sign, but the triangle and the quadrilateral have opposite signs.

We now check the decomposition of the identity map. If it is decomposed as a triangle and a quadrilateral, we see that they are of the same sign, and so we obtain a positive domain. If it is decomposed as a pentagon and a hexagon, we see that the composite of the straightened rectangles is negative by Property (2) of Definition 4.1, but the right pentagon and its straightening have opposite signs; this means that the overall domain is also positive. \square

The proof of Proposition 4.3 is completed by combining Lemmas 4.4, 4.5, 4.6 and 4.7.

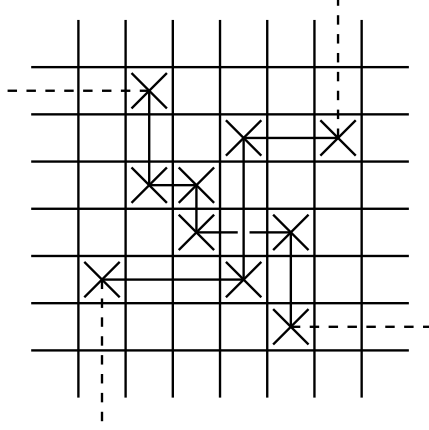


FIGURE 5.1. The grid diagram G of an oriented link L near a crossing. The 6×6 block of cells in the center is the block associated to this crossing.

5. ITERATION OF THE SKEIN EXACT TRIANGLE

Let G_0, G_1, G_2 be grid diagrams that are identical except near a point, as indicated in Figure 3.1. In Sections 3 and 4, we constructed the maps $f_k: C(G_k) \rightarrow C(G_{k+1})$ and $\varphi_k: C(G_k) \rightarrow C(G_{k+2})$ that satisfy Lemma 3.2 (or Lemma 4.4). If we unravel the proof of Lemma 3.2 (or Lemma 4.4), we see that it actually implies that $C(G_0)$ is quasi-isomorphic to the mapping cone of $f_1: C(G_1) \rightarrow C(G_2)$, where the quasi-isomorphism is given by $f_0 + \varphi_0: C(G_0) \rightarrow C(G_1) \oplus C(G_2)$.

We now wish to iterate this quasi-isomorphism to obtain a cube of resolutions that computes the same homology.

Let G be a grid diagram for an oriented link L , and let the crossings in G be numbered from 1 to m . By applying stabilisation and commutation as described in [Cro95, Dyn06, MOST07], we can require that

- (1) Near every crossing, the diagram G is as indicated in Figure 5.1. For the i -th crossing, the associated 6×6 block of cells illustrated is referred to as the i -th block;
- (2) If $i \neq j$, then the i -th block and the j -th block occupy disjoint rows and disjoint columns.

To each sequence k_1, k_2, \dots, k_m , where $k_i \in \mathbb{Z}/3\mathbb{Z}$ for $1 \leq i \leq m$, we associate a grid diagram G_{k_1, \dots, k_m} . The diagram G_{k_1, \dots, k_m} is obtained from G by replacing the i -th block by the appropriate 6×6 block as in Figure 3.1 (where the central 4×4 block is shown), depending on the value of k_i . In particular, $G_{0, \dots, 0} = G$. Let C_{k_1, \dots, k_m} be the associated chain complex of G_{k_1, \dots, k_m} , equipped with the differential map. For $1 \leq i \leq m$, we let the edge map

$$f_{k_1, \dots, k_m}^i: C_{k_1, \dots, k_{i-1}, k_i, k_{i+1}, \dots, k_m} \rightarrow C_{k_1, \dots, k_{i-1}, k_i+1, k_{i+1}, \dots, k_m}$$

be the map f_k defined in Section 3 (over \mathbb{F}_2) or Section 4 (over \mathbb{Z}); this is well defined, since the two chain complexes differ only near a crossing. Analogously, we have the map

$$\varphi_{k_1, \dots, k_m}^i: C_{k_1, \dots, k_{i-1}, k_i, k_{i+1}, \dots, k_m} \rightarrow C_{k_1, \dots, k_{i-1}, k_i+2, k_{i+1}, \dots, k_m},$$

which is just the map φ_k defined earlier.

The chain complexes with $k_i \in \{1, 2\}$ are each associated to a grid diagram in which all crossings have been resolved. We define the *cube of resolutions* of G to be the complex

$$(\mathrm{CR}(G), \partial_{\mathrm{CR}}) = \left(\bigoplus_{k_i \in \{1, 2\}} C_{k_1, \dots, k_m}, \sum_{k_i \in \{1, 2\}} \left(\partial_{k_1, \dots, k_m} + \sum_{j \text{ s.t. } k_j = 1} f_{k_1, \dots, k_m}^j \right) \right).$$

The case when there are two crossings is illustrated below:

$$\begin{array}{ccccc} & & \varphi_{0,0}^2 & & \\ & \nearrow & & \searrow & \\ C_{0,0} & \xrightarrow{f_{0,0}^2} & C_{0,1} & \xrightarrow{f_{0,1}^2} & C_{0,2} \\ & \searrow & \downarrow f_{0,1}^1 & \downarrow f_{0,2}^1 & \nearrow \\ & & C_{1,1} & \xrightarrow{f_{1,1}^2} & C_{1,2} \\ & \nearrow & \downarrow f_{1,1}^1 & \downarrow f_{1,2}^1 & \searrow \\ & & C_{2,1} & \xrightarrow{f_{2,1}^2} & C_{2,2} \end{array}$$

$\varphi_{0,1}^1$ on the left, $\varphi_{0,2}^1$ on the right

The cube of resolutions $\mathrm{CR}(G)$ consists of the 2×2 square on the lower right. In this context, our claim is that $C_{0,0}$ is quasi-isomorphic to the mapping cone of $f_{0,1}^2$ via $f_{0,0}^2 + \varphi_{0,0}^2$, which is in turn quasi-isomorphic to $\mathrm{CR}(G)$ via $f_{0,1}^1 + f_{0,2}^1 + \varphi_{0,1}^1 + \varphi_{0,2}^1$. Over \mathbb{F}_2 , the key to proving this claim is in the fact that the maps in the diagram commute. This immediately implies that

- (1) the cube of resolutions $\mathrm{CR}(G)$ is a chain complex;
- (2) the sum $f_{0,1}^1 + f_{0,2}^1 + \varphi_{0,1}^1 + \varphi_{0,2}^1$ is a chain map from the mapping cone of $f_{0,1}^2$ to the cube of resolutions $\mathrm{CR}(G)$; and
- (3) this chain map is a quasi-isomorphism.

(To see the last statement, observe that if $f: C_1 \rightarrow C_2$ and $f': C'_1 \rightarrow C'_2$ are quasi-isomorphisms, and if there exist maps $g_1: C_1 \rightarrow C'_1$ and $g_2: C_2 \rightarrow C'_2$ so that the diagram

$$\begin{array}{ccc} C_1 & \xrightarrow{f} & C_2 \\ g_1 \downarrow & & \downarrow g_2 \\ C'_1 & \xrightarrow{f'} & C'_2 \end{array}$$

commutes, then $f + f'$ is a quasi-isomorphism between the mapping cone of g_1 and that of g_2 .)

The general case is similar; to be precise, our claim is the following.

Proposition 5.1. *Let \mathbb{F}_2 be the base ring. The cube of resolutions $\mathrm{CR}(G)$ is in fact a chain complex. Moreover, it is quasi-isomorphic to $C(G)$.*

As mentioned, the main ingredient in proving Proposition 5.1 is the following lemma.

Lemma 5.2. *All maps involved commute. Precisely,*

$$\begin{aligned} f_{k_1, \dots, k_{i_1}+1, \dots, k_m}^{i_2} \circ f_{k_1, \dots, k_{i_1}, \dots, k_m}^{i_1} &= f_{k_1, \dots, k_{i_2}+1, \dots, k_m}^{i_1} \circ f_{k_1, \dots, k_{i_2}, \dots, k_m}^{i_2} \cdot \\ \varphi_{k_1, \dots, k_{i_1}+1, \dots, k_m}^{i_2} \circ f_{k_1, \dots, k_{i_1}, \dots, k_m}^{i_1} &= f_{k_1, \dots, k_{i_2}+2, \dots, k_m}^{i_1} \circ \varphi_{k_1, \dots, k_{i_2}, \dots, k_m}^{i_2} \cdot \end{aligned}$$

Proof. Inspecting the 6×6 block in Figure 5.1, we see that there is an X near each corner of the block, and so each allowed polygon defined in Section 3 counted in a chain map or a chain homotopy can only leave the block either horizontally or vertically. If it leaves the block horizontally, then it is contained in the rows that the block spans; if it leaves the block vertically, then it is contained in the columns that the block spans. This shows that if two rectangle-like polygons from two different crossings share a corner, one must be long and horizontal, and the other long and vertical; in such cases, the composite domain always has an obvious alternative decomposition. If at least one of the two polygons from two distinct crossings is triangle-like, then they can only be disjoint or have overlapping interiors. \square

Proof of Proposition 5.1. Exactly as in the case with two crossings, Lemma 5.2 implies that the cube of resolutions is indeed a chain complex, and that all appropriate maps are chain maps. We proceed by induction; at each step, we claim that the chain complexes

$$\left(\bigoplus_{k_i \in \{1,2\}} C_{0, \dots, 0, k_{t+1}, \dots, k_m}, \sum_{k_i \in \{1,2\}} \left(\partial_{0, \dots, 0, k_{t+1}, \dots, k_m} + \sum_{j \text{ s.t. } k_j=1} f_{0, \dots, 0, k_{t+1}, \dots, k_m}^j \right) \right)$$

and

$$\left(\bigoplus_{k_i \in \{1,2\}} C_{0, \dots, 0, k_t, \dots, k_m}, \sum_{k_i \in \{1,2\}} \left(\partial_{0, \dots, 0, k_t, \dots, k_m} + \sum_{j \text{ s.t. } k_j=1} f_{0, \dots, 0, k_t, \dots, k_m}^j \right) \right)$$

are quasi-isomorphic. The quasi-isomorphism is given by

$$\sum_{k_i \in \{1,2\}} f_{(0, \dots, 0, k_{t+1}, \dots, k_m)}^t + \sum_{k_i \in \{1,2\}} \varphi_{(0, \dots, 0, k_{t+1}, \dots, k_m)}^t.$$

This map is a quasi-isomorphism by the induction hypothesis and by the comment after (3) in the case with two crossings above. \square

Over \mathbb{Z} , the situation is slightly more complicated: We would like the entire diagram to anti-commute rather than to commute. The maps f^i are indeed anti-chain maps; in fact, the maps $f^i + \varphi^i$ are also anti-chain maps between mapping cones. (The subscripts have been suppressed for simplicity.) However, whenever $i_1 \neq i_2$, the maps with superscript i_1 do not anti-commute with those with superscript i_2 . Looking more carefully at our definitions, we see that if we denote by ρ^i maps defined by rectangle-like polygons and by τ^i maps defined by triangle-like polygons, then

- (1) $\rho^{i_2} \circ \rho^{i_1} = -\rho^{i_2} \circ \rho^{i_1}$;
- (2) $\rho^{i_2} \circ \tau^{i_1} = \tau^{i_2} \circ \rho^{i_1}$;
- (3) $\tau^{i_2} \circ \rho^{i_1} = \rho^{i_2} \circ \tau^{i_1}$;
- (4) $\tau^{i_2} \circ \tau^{i_1} = \tau^{i_2} \circ \tau^{i_1}$,

whenever $i_1 \neq i_2$. Property (1) follows from Definition 4.1 (1), while Properties (2) to (4) follow from the fact that triangle-like polygons always have their corners

inside the 6×6 block associated to a crossing, and thus can never share a corner with another polygon from another crossing.

To circumvent this problem, we modify the maps f^i and φ^i by sprinkling appropriate signs on τ^i . Observe that the entire discussion in Section 4 would have held true, had we made the definitions

$$\epsilon_k^{\mathcal{T}}(p) = -\operatorname{sgn}(\mathbf{x}), \quad \epsilon_k^{\mathcal{Q}}(p) = -\operatorname{sgn}(\mathbf{x}),$$

instead of

$$\epsilon_k^{\mathcal{T}}(p) = \operatorname{sgn}(\mathbf{x}), \quad \epsilon_k^{\mathcal{Q}}(p) = \operatorname{sgn}(\mathbf{x}).$$

Indeed, while Type I and Type IV domains are not affected by this change, the signs of Type II and Type III domains are flipped; it remains to observe that a Type II or Type III domain always admits an alternative decomposition that is also Type II or Type III. Thus, for a fixed sequence k_1, \dots, k_m and a fixed i , making the modifications

$$f_{k_1, \dots, k_m}^i = \mathcal{P}_{k_1, \dots, k_m}^i - \mathcal{T}_{k_1, \dots, k_m}^i$$

and

$$\varphi_{k_1, \dots, k_m}^i = \mathcal{H}_{k_1, \dots, k_m}^i - \mathcal{Q}_{k_1, \dots, k_m}^i$$

preserves the quasi-isomorphism corresponding to the i -th crossing.

We make these modifications to f_{k_1, \dots, k_m}^i and $\varphi_{k_1, \dots, k_m}^i$ whenever

$$\# \{j \mid j > i \text{ and } k_j = 1\}$$

is odd. In the two-crossing case, the signs of the triangle-like polygons in $f_{0,1}^1, f_{1,1}^1$ and $\varphi_{0,1}^1$ are changed. It can be readily seen that now the diagram anti-commutes. In general, for every rectangle in a similar diagram, we are making a sign change in triangle-like polygons for exactly one or three sides of the rectangle, and so now the diagram anti-commutes. The rest of the discussion over \mathbb{F}_2 carries through to the situation over \mathbb{Z} . We have proven:

Proposition 5.3. *Let \mathbb{Z} be the base ring. The cube of resolutions $\operatorname{CR}(G)$ is in fact a chain complex. Moreover, it is quasi-isomorphic to $C(G)$.*

Corollary 1.3 follows from Propositions 5.1 and 5.3.

6. QUASI-ALTERNATING LINKS

We now describe an application of the skein exact triangle. To begin, we must first define the δ -grading on knot Floer homology. The δ -grading is closely related to the Maslov and Alexander gradings; in view of that, in this section we revert to the traditional notation with both O 's and X 's, and denote the set of O 's by \mathbb{O} and that of X 's by \mathbb{X} .

The following formulation is found in [MOST07]. Given two collections A and B of finitely many points in the plane, let

$$\begin{aligned} \mathcal{J}(A, B) = & \frac{1}{2} \# \{((a_1, a_2), (b_1, b_2)) \in A \times B \mid a_1 < b_1 \text{ and } a_2 < b_2\} \\ & + \frac{1}{2} \# \{(a_1, a_0), (b_1, b_2)) \in A \times B \mid b_1 < a_1 \text{ and } b_2 < a_2\}. \end{aligned}$$

Treating $\mathbf{x} \in \mathbf{S}(G)$ as a collection of points with integer coordinates in a fundamental domain for \mathbb{T} , and similarly \mathbb{O} and \mathbb{X} as collections of points in the plane with half-integer coordinates, the Maslov grading of a generator is given by

$$M(\mathbf{x}) = \mathcal{J}(\mathbf{x}, \mathbf{x}) - 2\mathcal{J}(\mathbf{x}, \mathbb{O}) + \mathcal{J}(\mathbb{O}, \mathbb{O}) + 1,$$

while the Alexander grading is given by

$$A(\mathbf{x}) = \mathcal{J}(\mathbf{x}, \mathbb{X}) - \mathcal{J}(\mathbf{x}, \mathbb{O}) - \frac{1}{2}\mathcal{J}(\mathbb{X}, \mathbb{X}) + \frac{1}{2}\mathcal{J}(\mathbb{O}, \mathbb{O}) - \frac{n-1}{2},$$

where n is the size of the grid diagram. Now the δ -grading is just

$$\delta(\mathbf{x}) = A(\mathbf{x}) - M(\mathbf{x});$$

in other words, we have

$$\delta(\mathbf{x}) = -\mathcal{J}(\mathbf{x}, \mathbf{x}) + \mathcal{J}(\mathbf{x}, \mathbb{X}) + \mathcal{J}(\mathbf{x}, \mathbb{O}) - \frac{1}{2}\mathcal{J}(\mathbb{X}, \mathbb{X}) - \frac{1}{2}\mathcal{J}(\mathbb{O}, \mathbb{O}) - \frac{n+1}{2}.$$

These gradings do not depend on the choice of the fundamental domain; moreover, they agree with the original definitions in terms of pseudo-holomorphic representatives.

It has been observed that, for many classes of links, the knot Floer homology over $R = \mathbb{F}_2$ or \mathbb{Z} is a free R -module supported in only one δ -grading, which motivates the following definition [Ras03, Ras05, MO08]:

Definition 6.1. Let the base ring be $R = \mathbb{F}_2$ or \mathbb{Z} . A link L is *Floer homologically thin* over R if $\widehat{\text{HFK}}(L)$ is a free R -module supported in only one δ -grading. If in addition the δ -grading equals $-\sigma(L)/2$, where $\sigma(L)$ is the signature of the link, then we say that L is *Floer homologically σ -thin*.

In [MO08], Manolescu and Ozsváth show that a class of links, which is a natural generalisation of alternating knots, has the homologically σ -thin property over \mathbb{F}_2 . Precisely, we recall the following definition from [OS05]:

Definition 6.2. The set of *quasi-alternating links* \mathcal{Q} is the smallest set of links satisfying the following properties:

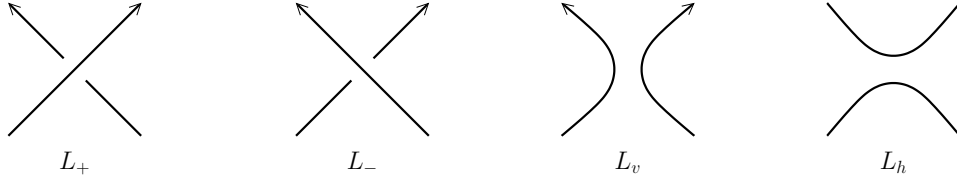
- (1) The unknot is in \mathcal{Q} .
- (2) If L_∞ is a link that admits a projection with a crossing such that
 - (a) both resolutions L_0 and L_1 at that crossing are in \mathcal{Q} ; and
 - (b) $\det(L_\infty) = \det(L_0) + \det(L_1)$,
 then L_∞ is in \mathcal{Q} .

The result of Manolescu and Ozsváth is then the following statement:

Theorem 6.3 (Manolescu–Ozsváth). *Let \mathbb{F}_2 be the base ring. Quasi-alternating links are Floer homologically σ -thin.*

The proof of the theorem is essentially an application of Manolescu’s unoriented skein exact triangle; the main work is in tracking the changes in the δ -grading of the maps involved. In that context, the δ -grading is given in terms of pseudo-holomorphic representatives; but the same idea works in the current context as well: With grid diagrams, we may similarly track the changes in the δ -grading, defined by the formula above. Of course, in our case, we will be proving the result for $\widehat{\text{HFG}}$ of a link instead of $\widehat{\text{HFK}}$. Since we have been working over both \mathbb{F}_2 and \mathbb{Z} , we will have proven Corollary 1.4, which is a strengthened version of Theorem 6.3.

To begin, fix a crossing c_0 in the planar diagram of a link L_∞ . Let L_+ be the link with a positive crossing at c_0 , and L_- the link with a negative crossing; then either $L_\infty = L_+$ or $L_\infty = L_-$. Let L_h and L_v be the unoriented and oriented resolutions of L_∞ at c_0 respectively, and choose an arbitrary orientation for L_h .

FIGURE 6.1. L_+ , L_- , L_h and L_v near a point.

This is illustrated in Figure 6.1. Comparing with Figure 1.1, if $L_\infty = L_+$, then $L_0 = L_h$ and $L_1 = L_v$; if instead $L_\infty = L_-$, then $L_0 = L_v$ and $L_1 = L_h$.

Denote by D_+, D_-, D_v, D_h the planar diagrams of L_+, L_-, L_v, L_h , differing from each other only at c_0 . The following lemma is used in [MO08]; for L_+ , the first equality is proven by Murasugi in [Mur65], while the second is also inspired by a result of Murasugi from [Mur70]. The equalities for L_- are similarly obtained.

Lemma 6.4. *Suppose that $\det(L_v), \det(L_h) > 0$. Let e denotes the difference between the number of negative crossings in D_h and the number of such crossings in D_+ . If $\det(L_+) = \det(L_v) + \det(L_h)$, then*

- (1) $\sigma(L_v) - \sigma(L_+) = 1$; and
- (2) $\sigma(L_h) - \sigma(L_+) = e$,

If $\det(L_-) = \det(L_v) + \det(L_h)$, then

- (1) $\sigma(L_v) - \sigma(L_-) = -1$; and
- (2) $\sigma(L_h) - \sigma(L_-) = e$.

Now we investigate the changes in the δ -grading in the maps f_k defined in Sections 3 and 4.

Lemma 6.5. *Let $\mathbf{x} \in \mathbf{S}(G)$ be a fixed generator in a grid diagram G . Then the following is true:*

- (1) *The boundary map changes the δ -grading of \mathbf{x} by $+1$.*
- (2) *Suppose two markers on adjacent columns, regardless of type, and viewed as a southwest–northeast pair, are as in Figure 6.2. If they are moved as indicated in the figure, then the δ -grading of \mathbf{x} changes by*
 - (a) $-1/2$ *if the component of \mathbf{x} on the β curve between the markers lies to the northeast of one marker and to the southwest of the other before the move (indicated in the diagrams by a solid point); and*
 - (b) $+1/2$ *otherwise (the component of \mathbf{x} indicated by a hollow point).*
- (3) *If the diagram G' is obtained from G by reversing the orientation of a component K of L , then the δ -grading of \mathbf{x} changes by $-\epsilon/2$, where ϵ is the difference between the number of negative crossings in G' and the number of such crossings in G .*

Proof. Recall that

$$\delta(\mathbf{x}) = -\mathcal{J}(\mathbf{x}, \mathbf{x}) + \mathcal{J}(\mathbf{x}, \mathbb{X}) + \mathcal{J}(\mathbf{x}, \mathbb{O}) - \frac{1}{2}\mathcal{J}(\mathbb{X}, \mathbb{X}) - \frac{1}{2}\mathcal{J}(\mathbb{O}, \mathbb{O}) - \frac{n+1}{2}.$$

Observe that $\mathcal{J}(A, B)$ is the number of southwest–northeast pairs between A and B , divided by two. Consider the following:

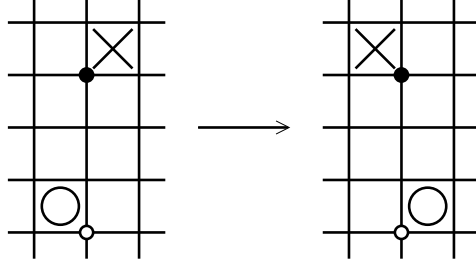


FIGURE 6.2. Moving two markers across a β curve. Observe that before the move, the solid point lies to the northeast of the O and to the southwest of the X , thus forming two southwest–northeast pairs with the markers that are destroyed in the move. The hollow point forms the same number of pairs before and after the move.

- (1) The boundary map counts only empty rectangles whose interiors do not intersect \mathbb{O} and \mathbb{X} , and so leaves all terms fixed, except $\mathcal{J}(\mathbf{x}, \mathbf{x})$. It destroys exactly one southwest–northeast pair, which is counted twice, and so the change in the δ -grading is $+1$.
- (2) Such a move always preserves $\mathcal{J}(\mathbf{x}, \mathbf{x})$ and changes $\mathcal{J}(\mathbb{X}, \mathbb{X}) + \mathcal{J}(\mathbb{O}, \mathbb{O})$ by -1 . If the component of \mathbf{x} on the β curve does not lie to the northeast of one marker and to the southwest of the other, then $\mathcal{J}(\mathbf{x}, \mathbb{X}) + \mathcal{J}(\mathbf{x}, \mathbb{O})$ is also fixed; otherwise, this quantity changes by -1 .
- (3) This operation always preserves $\mathcal{J}(\mathbf{x}, \mathbf{x})$ and $\mathcal{J}(\mathbf{x}, \mathbb{X}) + \mathcal{J}(\mathbf{x}, \mathbb{O})$. Suppose K encircles the regions R_1, \dots, R_m in the plane. If K traces the boundary of the region R_i in the anti-clockwise direction, then

$$\begin{aligned} & \# \{ \text{positive crossings in } R_i \} - \# \{ \text{negative crossings in } R_i \} \\ &= \#(\mathbb{X} \cap \text{Int } R_i) - \#(\mathbb{O} \cap \text{Int } R_i). \end{aligned}$$

Reversing the orientation of K reverses the signs of all these crossings. Thus, if K traces the boundary of all regions R_i in the anti-clockwise direction, then

$$\epsilon = \#(\mathbb{X} \cap \text{Int } R_i) - \#(\mathbb{O} \cap \text{Int } R_i).$$

Consider now the effect on $\mathcal{J}(\mathbb{X}, \mathbb{X}) + \mathcal{J}(\mathbb{O}, \mathbb{O})$: It is not hard to see that only southwest–northeast pairs between a marker in $\text{Int } R_i$ and another on ∂R_i are affected. Observe that the northeast-most marker and the southwest-most marker are both O 's; reversing the orientation of K destroys two southwest–northeast pairs for each $O \in \text{Int } R_i$ (counted twice), and creates two such pairs for each $X \in \text{Int } R_i$ (counted twice). This shows that the change in the quantity $\mathcal{J}(\mathbb{X}, \mathbb{X}) + \mathcal{J}(\mathbb{O}, \mathbb{O})$ is exactly ϵ . The case where K traces the boundary of some regions R_i in the clockwise direction is analogous.

This completes the proof of the lemma. □

The following is an easy consequence of Lemma 6.5 (1) and (2):

Lemma 6.6. *If G_k and G_{k+1} are grid presentations of two links with compatible orientations (so that G_k and G_{k+1} have compatible sets of O 's), then $f_k: G_k \rightarrow G_{k+1}$ changes the δ -grading by $+1/2$.*

Proof. In general, the map f_k can be thought of as consisting of a number of moves as described in Lemma 6.5 (2), possibly composed with an empty rectangle (i.e. the boundary map). When G_k and G_{k+1} are grid presentations of links with compatible orientations, the map f_k consists of only one such move. If the component of $\mathbf{x} \in \mathbf{S}(G_k)$ on the β curve between the two markers is as described in (2)(a), then the domain counted in f_k is a pentagon; otherwise, it is a triangle. In the former case, the pentagon can be thought of as a boundary map composed with the move in (2) (in either order), and so the total change in the δ -grading is $+1 - 1/2 = +1/2$. In the latter case, the resulting generator $\mathbf{y} \in \mathbf{S}(G_{k+1})$ is the corresponding generator of \mathbf{x} (i.e. they are canonically closest), and so the change in the δ -grading is simply $+1/2$. \square

We can now prove a graded version of Theorem 1.2:

Proposition 6.7. *Let the base ring be $R = \mathbb{F}_2$ or \mathbb{Z} . With respect to the δ -grading, there exist exact sequences*

$$\begin{aligned} \cdots \rightarrow \widehat{\text{HFG}}_{*-\frac{1}{2}}(L_v) \otimes V^{m-\ell_v} &\rightarrow \widehat{\text{HFG}}_*(L_+) \otimes V^{m-\ell_+} \\ &\rightarrow \widehat{\text{HFG}}_{*-\frac{e}{2}}(L_h) \otimes V^{m-\ell_h} \rightarrow \widehat{\text{HFG}}_{*-\frac{1}{2}+1}(L_1) \otimes V^{m-\ell_1} \rightarrow \cdots \end{aligned}$$

and

$$\begin{aligned} \cdots \rightarrow \widehat{\text{HFG}}_{*-\frac{e}{2}}(L_h) \otimes V^{m-\ell_h} &\rightarrow \widehat{\text{HFG}}_*(L_-) \otimes V^{m-\ell_-} \\ &\rightarrow \widehat{\text{HFG}}_{*+\frac{1}{2}}(L_v) \otimes V^{m-\ell_v} \rightarrow \widehat{\text{HFG}}_{*-\frac{e}{2}+1}(L_h) \otimes V^{m-\ell_h} \rightarrow \cdots, \end{aligned}$$

where V is a free module of rank 2 over R with grading zero, and where e is as in the statement of Lemma 6.4.

Proof. Suppose L_∞ has a positive crossing at c_0 , so that $L_+ = L_\infty$, $L_v = L_1$ and $L_0 = L_h$. Let G_0, G_1, G_2 be grid diagrams for L_∞, L_0, L_1 respectively, differing with each other only at c_0 as in Figure 3.1. Note that in Figure 3.1 only X 's are used as markers, whereas in the present context both X 's and O 's are used. Then we are to prove that in the exact sequence

$$\cdots \rightarrow \widehat{\text{HK}}(G_2) \xrightarrow{(f_2)*} \widehat{\text{HK}}(G_0) \xrightarrow{(f_0)*} \widehat{\text{HK}}(G_1) \xrightarrow{(f_1)*} \widehat{\text{HK}}(G_2) \rightarrow \cdots,$$

the map f_2 shifts the δ -grading by $+1/2$, f_0 by $-e/2$, and f_1 by $+(e+1)/2$.

Refer to Figure 6.3. Since L_1 and L_∞ have compatible orientations, Lemma 6.6 shows that the map f_2 shifts the δ -grading by $+1/2$.

Let us now focus on f_0 . The key steps are illustrated in Figure 6.4. The two strands of the link L_+ meeting at the crossing c_0 may belong to either one or two components of L_+ . If they belong to two different components, then we follow the two operations in the top row; otherwise, we follow the three operations in the bottom row.

Suppose the strands belong to different components; the first operation corresponds to reversing the orientation of a component, and the second to a usual f_0 map (from the new diagram to G_1). Notice that the two grid diagrams involved in this new f_0 map are for links with compatible orientations, so the δ -grading shift is just $+1/2$. By Lemma 6.5 (3), the first operation changes the δ -grading

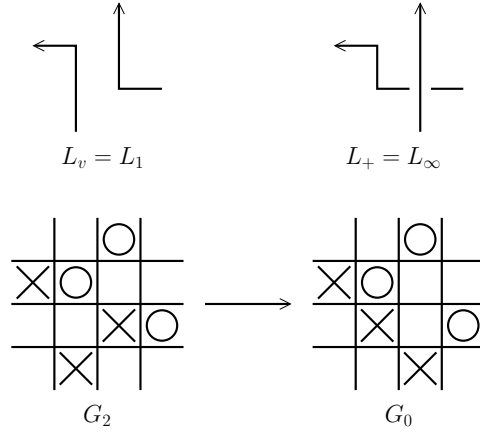


FIGURE 6.3. A straightforward application of Lemma 6.6 gives the δ -grading shift of f_2 .

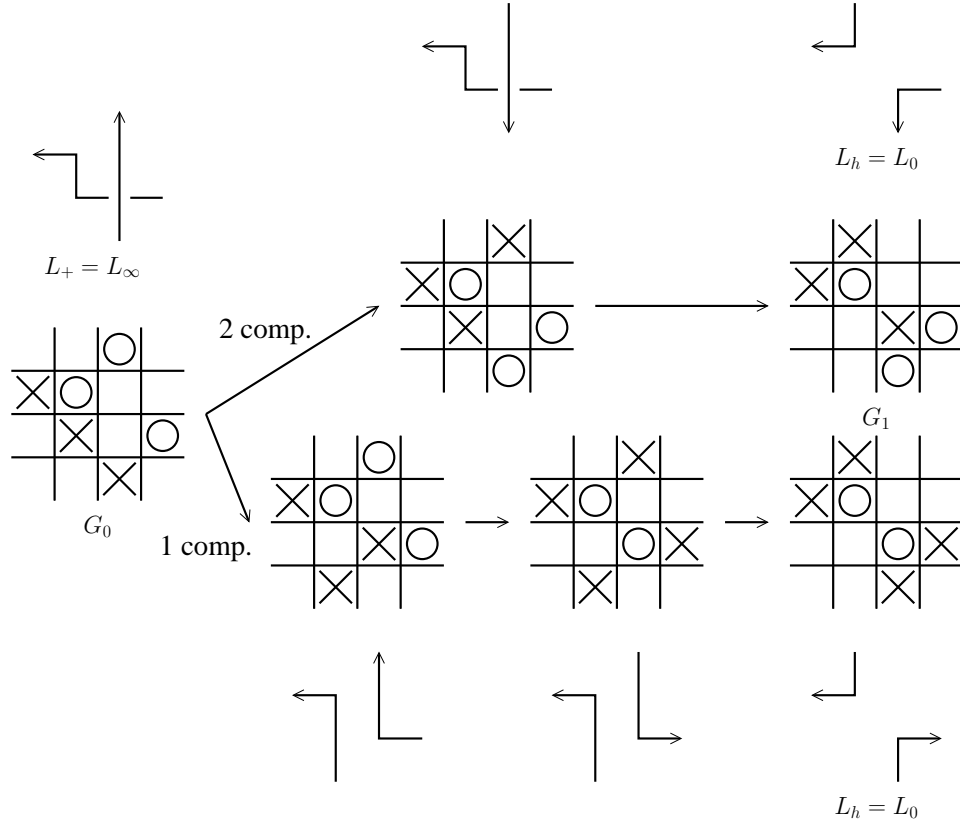


FIGURE 6.4. Computation of the δ -grading shift of f_0 . If the two strands meeting at c_0 belong to different components, the top row applies; otherwise, the bottom row applies.

by $-\epsilon/2$; observing that the resulting link has one more negative crossing than $L_0 = L_h$, we see that the $\epsilon = e + 1$. The total change in the δ -grading is therefore $-(e + 1)/2 + 1/2 = -e/2$.

Suppose now the strands belong to the same component; this case requires slightly more work. The second of the three operations corresponds to reversing the orientation of a link component, and its δ -grading change is readily computed to be $-e/2$. Notice that this operation is valid, since after the first operation, the two strands at the crossing now belong to different components of the link.

Position the grid diagram so that the bottom left of the part shown is at the origin $(0, 0)$. We shall refer to the intersection points by their integer coordinates; the middle point of the portion shown is $(2, 2)$. Intersection points outside the range $[0, 3] \times [0, 3]$ are referred to by the obvious coordinates in the range; for example, what would be $(2, 4)$ and $(2, 5)$ are also referred to as $(2, 0)$.

By Lemma 6.5 (2), the first operation shifts the δ -grading by $-1/2$ if the component of \mathbf{x} on the central β curve is at $(2, 2)$, $(2, 3)$ or $(2, 0)$, and by $+1/2$ if it is at $(2, 1)$. Likewise, the third operation shifts the δ -grading by $-1/2$ if the component of \mathbf{x} is at $(2, 1)$, $(2, 2)$ or $(2, 3)$, and by $+1/2$ if it is at $(2, 0)$. Thus, the sum of the δ -grading shift from the first and the third operations is 0 if the component of \mathbf{x} is at $(2, 0)$ or $(2, 1)$, and -1 if it is at $(2, 2)$ or $(2, 3)$. Observe that if the component is at $(2, 0)$ or $(2, 1)$ during the operations, then the domain counted is a triangle; thus, the resulting generator \mathbf{y} is the corresponding generator. On the other hand, if the component is at $(2, 2)$ or $(2, 3)$ during the operations, then the domain counted is a pentagon, which can be viewed as the composition of a boundary map and the three operations (in either order); thus, a δ -grading shift of $+1$ must be added. In either case, the total change in the δ -grading is $-e/2 + 0 = -e/2$.

Finally, a calculation analogous to that for f_0 can be done for f_1 , and we obtain, in this case, that the change in the δ -grading is $+(e + 1)/2$.

The case when $L_\infty = L_-$ has a negative crossing at c_0 is similar. \square

We can now conclude:

Proposition 6.8. *Let the base ring be $R = \mathbb{F}_2$ or \mathbb{Z} . Let L_∞ be a link and L_0, L_1 its two resolutions as in Figure 1.1. Suppose that $\det(L_0), \det(L_1) > 0$ and $\det(L_\infty) = \det(L_0) + \det(L_1)$. With respect to the δ -grading, there exists an exact sequence*

$$\begin{aligned} \cdots \rightarrow \widehat{\text{HFG}}_{*-\frac{\sigma(L_1)}{2}}(L_1) \otimes V^{m-\ell_1} &\rightarrow \widehat{\text{HFG}}_{*-\frac{\sigma(L_\infty)}{2}}(L_\infty) \otimes V^{m-\ell_\infty} \\ &\rightarrow \widehat{\text{HFG}}_{*-\frac{\sigma(L_0)}{2}}(L_0) \otimes V^{m-\ell_0} \rightarrow \widehat{\text{HFG}}_{*-\frac{\sigma(L_1)}{2}+1}(L_1) \otimes V^{m-\ell_1} \rightarrow \cdots, \end{aligned}$$

where V is a free module of rank 2 over R with grading zero.

Proof. This is just a restatement of Proposition 6.7, taking into account the result of Lemma 6.4. \square

Proof of Corollary 1.4. By definition, every quasi-alternating link has non-zero determinant. It can easily be checked that the unknot is homologically σ -thin. If L_0 and L_1 are resolutions of L_∞ that are quasi-alternating, then by induction, L_0 and L_1 are homologically σ -thin. The exact sequence in Proposition 6.8 collapses into short exact sequences, all but one of which are zero. Thus L_∞ is also homologically σ -thin. \square

REFERENCES

- [Bal11] John A. Baldwin, *On the spectral sequence from Khovanov homology to Heegaard Floer homology*, Int. Math. Res. Not. IMRN (2011), no. 15, 3426–3470. MR 2822178 (2012g:57021)
- [BL12] John A. Baldwin and Adam Simon Levine, *A combinatorial spanning tree model for knot Floer homology*, Adv. Math. **231** (2012), no. 3-4, 1886–1939. MR 2964628
- [BN02] Dror Bar-Natan, *On Khovanov’s categorification of the Jones polynomial*, Algebr. Geom. Topol. **2** (2002), 337–370 (electronic). MR 1917056 (2003h:57014)
- [Cro95] Peter R. Cromwell, *Embedding knots and links in an open book. I. Basic properties*, Topology Appl. **64** (1995), no. 1, 37–58. MR 1339757 (96g:57006)
- [Dyn06] I. A. Dynnikov, *Arc-presentations of links: monotonic simplification*, Fund. Math. **190** (2006), 29–76. MR 2232855 (2007e:57006)
- [Kho00] Mikhail Khovanov, *A categorification of the Jones polynomial*, Duke Math. J. **101** (2000), no. 3, 359–426. MR 1740682 (2002j:57025)
- [Kho02] ———, *A functor-valued invariant of tangles*, Algebr. Geom. Topol. **2** (2002), 665–741 (electronic). MR 1928174 (2004d:57016)
- [LOT] Robert Lipshitz, Peter S. Ozsváth, and Dylan P. Thurston, *Bordered Floer homology and the branched double cover I*, Preprint, <http://arxiv.org/abs/1011.0499>.
- [Man07] Ciprian Manolescu, *An unoriented skein exact triangle for knot Floer homology*, Math. Res. Lett. **14** (2007), no. 5, 839–852. MR 2350128 (2008m:57074)
- [MO08] Ciprian Manolescu and Peter Ozsváth, *On the Khovanov and knot Floer homologies of quasi-alternating links*, Proceedings of Gökova Geometry-Topology Conference 2007, Gökova Geometry/Topology Conference (GGT), Gökova, 2008, pp. 60–81. MR 2509750 (2010k:57029)
- [MOS09] Ciprian Manolescu, Peter Ozsváth, and Sucharit Sarkar, *A combinatorial description of knot Floer homology*, Ann. of Math. (2) **169** (2009), no. 2, 633–660. MR 2480614 (2009k:57047)
- [MOST07] Ciprian Manolescu, Peter Ozsváth, Zoltán Szabó, and Dylan Thurston, *On combinatorial link Floer homology*, Geom. Topol. **11** (2007), 2339–2412. MR 2372850 (2009c:57053)
- [Mur65] Kunio Murasugi, *On a certain numerical invariant of link types*, Trans. Amer. Math. Soc. **117** (1965), 387–422. MR 0171275 (30 #1506)
- [Mur70] ———, *On the signature of links*, Topology **9** (1970), 283–298. MR 0261585 (41 #6198)
- [OS04a] Peter Ozsváth and Zoltán Szabó, *Holomorphic disks and knot invariants*, Adv. Math. **186** (2004), no. 1, 58–116. MR 2065507 (2005e:57044)
- [OS04b] ———, *Holomorphic disks and topological invariants for closed three-manifolds*, Ann. of Math. (2) **159** (2004), no. 3, 1027–1158. MR 2113019 (2006b:57016)
- [OS05] ———, *On the Heegaard Floer homology of branched double-covers*, Adv. Math. **194** (2005), no. 1, 1–33. MR 2141852 (2006e:57041)
- [OS08] ———, *Holomorphic disks, link invariants and the multi-variable Alexander polynomial*, Algebr. Geom. Topol. **8** (2008), no. 2, 615–692. MR 2443092 (2010h:57023)
- [Ras03] Jacob Andrew Rasmussen, *Floer homology and knot complements*, Ph.D. thesis, Harvard University, 2003, <http://arxiv.org/abs/math/0306378>.
- [Ras05] Jacob Rasmussen, *Knot polynomials and knot homologies*, Geometry and topology of manifolds, Fields Inst. Commun., vol. 47, Amer. Math. Soc., Providence, RI, 2005, pp. 261–280. MR 2189938 (2006i:57029)
- [Sar11] Sucharit Sarkar, *A note on sign conventions in link Floer homology*, Quantum Topol. **2** (2011), no. 3, 217–239. MR 2812456 (2012f:57033)

DEPARTMENT OF MATHEMATICS, COLUMBIA UNIVERSITY, NEW YORK, NY 10027, USA

E-mail address: cmmwong@math.columbia.edu

URL: <http://math.columbia.edu/~cmmwong/>